IMMUNOHISTOCHEMICAL STUDY OF CONNEXIN43 AND ASTROCYTIC GAP JUNCTIONS IN NORMAL AND INJURED SPINAL CORD OF RAT

BY

UTA NICOLA FRANKENSTEIN

A Thesis
submitted to the Faculty of Graduate Studies
in Partial Fulfillment of the Requirements
for the Degree of

MASTER OF SCIENCE

Department of Physiology
University of Manitoba
Winnipeg, Manitoba

ISBN 0-612-13131-9

Name _____

Dissertation Abstracts International is arranged by broad, general subject categories. Please select the one subject which most nearly describes the content of your dissertation. Enter the corresponding four-digit code in the spaces provided.

NEUROSCIENCE
SUBJECT TERM

0317
SUBJECT CODE

U·M·I

Subject Categories

THE HUMANITIES AND SOCIAL SCIENCES

COMMUNICATIONS AND THE ARTS
Architecture 0729
Art History 0377
Cinema 0900
Dance 0378
Fine Arts 0357
Information Science 0723
Journalism 0391
Library Science 0399
Mass Communications 0708
Music 0413
Speech Communication 0459
Theater 0465

EDUCATION
General 0515
Administration 0514
Adult and Continuing 0516
Agricultural 0517
Art 0273
Bilingual and Multicultural 0282
Business 0688
Community College 0275
Curriculum and Instruction 0727
Early Childhood 0518
Elementary 0524
Finance 0277
Guidance and Counseling 0519
Health 0680
Higher 0745
History of 0520
Home Economics 0278
Industrial 0521
Language and Literature 0279
Mathematics 0280
Music 0522
Philosophy of 0998
Physical 0523
Psychology 0525
Reading 0535
Religious 0527
Sciences 0714
Secondary 0533
Social Sciences 0534
Sociology of 0340
Special 0529
Teacher Training 0530
Technology 0710
Tests and Measurements 0288
Vocational 0747

LANGUAGE, LITERATURE AND LINGUISTICS
Language
- General 0679
- Ancient 0289
- Linguistics 0290
- Modern 0291

Literature
- General 0401
- Classical 0294
- Comparative 0295
- Medieval 0297
- Modern 0298
- African 0316
- American 0591
- Asian 0305
- Canadian (English) 0352
- Canadian (French) 0355
- English 0593
- Germanic 0311
- Latin American 0312
- Middle Eastern 0315
- Romance 0313
- Slavic and East European 0314

PHILOSOPHY, RELIGION AND THEOLOGY
Philosophy 0422
Religion
- General 0318
- Biblical Studies 0321
- Clergy 0319
- History of 0320
- Philosophy of 0322

Theology 0469

SOCIAL SCIENCES
American Studies 0323
Anthropology
- Archaeology 0324
- Cultural 0326
- Physical 0327

Business Administration
- General 0310
- Accounting 0272
- Banking 0770
- Management 0454
- Marketing 0338

Canadian Studies 0385
Economics
- General 0501
- Agricultural 0503
- Commerce-Business 0505
- Finance 0508
- History 0509
- Labor 0510
- Theory 0511

Folklore 0358
Geography 0366
Gerontology 0351
History
- General 0578
- Ancient 0579
- Medieval 0581
- Modern 0582
- Black 0328
- African 0331
- Asia, Australia and Oceania 0332
- Canadian 0334
- European 0335
- Latin American 0336
- Middle Eastern 0333
- United States 0337

History of Science 0585
Law 0398
Political Science
- General 0615
- International Law and Relations 0616
- Public Administration 0617

Recreation 0814
Social Work 0452
Sociology
- General 0626
- Criminology and Penology 0627
- Demography 0938
- Ethnic and Racial Studies 0631
- Individual and Family Studies 0628
- Industrial and Labor Relations 0629
- Public and Social Welfare 0630
- Social Structure and Development 0700
- Theory and Methods 0344

Transportation 0709
Urban and Regional Planning 0999
Women's Studies 0453

THE SCIENCES AND ENGINEERING

BIOLOGICAL SCIENCES
Agriculture
- General 0473
- Agronomy 0285
- Animal Culture and Nutrition 0475
- Animal Pathology 0476
- Food Science and Technology 0359
- Forestry and Wildlife 0478
- Plant Culture 0479
- Plant Pathology 0480
- Plant Physiology 0817
- Range Management 0777
- Wood Technology 0746

Biology
- General 0306
- Anatomy 0287
- Biostatistics 0308
- Botany 0309
- Cell 0379
- Ecology 0329
- Entomology 0353
- Genetics 0369
- Limnology 0793
- Microbiology 0410
- Molecular 0307
- Neuroscience 0317
- Oceanography 0416
- Physiology 0433
- Radiation 0821
- Veterinary Science 0778
- Zoology 0472

Biophysics
- General 0786
- Medical 0760

EARTH SCIENCES
Biogeochemistry 0425
Geochemistry 0996
Geodesy 0370
Geology 0372
Geophysics 0373
Hydrology 0388
Mineralogy 0411
Paleobotany 0345
Paleoecology 0426
Paleontology 0418
Paleozoology 0985
Palynology 0427
Physical Geography 0368
Physical Oceanography 0415

HEALTH AND ENVIRONMENTAL SCIENCES
Environmental Sciences 0768
Health Sciences
- General 0566
- Audiology 0300
- Chemotherapy 0992
- Dentistry 0567
- Education 0350
- Hospital Management 0769
- Human Development 0758
- Immunology 0982
- Medicine and Surgery 0564
- Mental Health 0347
- Nursing 0569
- Nutrition 0570
- Obstetrics and Gynecology 0380
- Occupational Health and Therapy 0354
- Ophthalmology 0381
- Pathology 0571
- Pharmacology 0419
- Pharmacy 0572
- Physical Therapy 0382
- Public Health 0573
- Radiology 0574
- Recreation 0575
- Speech Pathology 0460
- Toxicology 0383

Home Economics 0386

PHYSICAL SCIENCES
Pure Sciences
Chemistry
- General 0485
- Agricultural 0749
- Analytical 0486
- Biochemistry 0487
- Inorganic 0488
- Nuclear 0738
- Organic 0490
- Pharmaceutical 0491
- Physical 0494
- Polymer 0495
- Radiation 0754

Mathematics 0405
Physics
- General 0605
- Acoustics 0986
- Astronomy and Astrophysics 0606
- Atmospheric Science 0608
- Atomic 0748
- Electronics and Electricity 0607
- Elementary Particles and High Energy 0798
- Fluid and Plasma 0759
- Molecular 0609
- Nuclear 0610
- Optics 0752
- Radiation 0756
- Solid State 0611

Statistics 0463

Applied Sciences
Applied Mechanics 0346
Computer Science 0984
Engineering
- General 0537
- Aerospace 0538
- Agricultural 0539
- Automotive 0540
- Biomedical 0541
- Chemical 0542
- Civil 0543
- Electronics and Electrical 0544
- Heat and Thermodynamics 0348
- Hydraulic 0545
- Industrial 0546
- Marine 0547
- Materials Science 0794
- Mechanical 0548
- Metallurgy 0743
- Mining 0551
- Nuclear 0552
- Packaging 0549
- Petroleum 0765
- Sanitary and Municipal 0554
- System Science 0790

Geotechnology 0428
Operations Research 0796
Plastics Technology 0795
Textile Technology 0994

PSYCHOLOGY
General 0621
Behavioral 0384
Clinical 0622
Developmental 0620
Experimental 0623
Industrial 0624
Personality 0625
Physiological 0989
Psychobiology 0349
Psychometrics 0632
Social 0451

Nom _____

Dissertation Abstracts International est organisé en catégories de sujets. Veuillez s.v.p. choisir le sujet qui décrit le mieux votre thèse et inscrivez le code numérique approprié dans l'espace réservé ci-dessous.

_____ ☐☐☐ U·M·I

SUJET — CODE DE SUJET

Catégories par sujets

HUMANITÉS ET SCIENCES SOCIALES

COMMUNICATIONS ET LES ARTS
Architecture 0729
Beaux-arts 0357
Bibliothéconomie 0399
Cinéma 0900
Communication verbale 0459
Communications 0708
Danse 0378
Histoire de l'art 0377
Journalisme 0391
Musique 0413
Sciences de l'information 0723
Théâtre 0465

ÉDUCATION
Généralités 515
Administration 0514
Art 0273
Collèges communautaires 0275
Commerce 0688
Économie domestique 0278
Éducation permanente 0516
Éducation préscolaire 0518
Éducation sanitaire 0680
Enseignement agricole 0517
Enseignement bilingue et multiculturel 0282
Enseignement industriel 0521
Enseignement primaire. 0524
Enseignement professionnel 0747
Enseignement religieux 0527
Enseignement secondaire 0533
Enseignement spécial 0529
Enseignement supérieur 0745
Évaluation 0288
Finances 0277
Formation des enseignants 0530
Histoire de l'éducation 0520
Langues et littérature 0279
Lecture 0535
Mathématiques 0280
Musique 0522
Orientation et consultation 0519
Philosophie de l'éducation 0998
Physique 0523
Programmes d'études et enseignement 0727
Psychologie 0525
Sciences 0714
Sciences sociales 0534
Sociologie de l'éducation 0340
Technologie 0710

LANGUE, LITTÉRATURE ET LINGUISTIQUE
Langues
- Généralités 0679
- Anciennes 0289
- Linguistique 0290
- Modernes 0291

Littérature
- Généralités 0401
- Anciennes 0294
- Comparée 0295
- Médiévale 0297
- Moderne 0298
- Africaine 0316
- Américaine 0591
- Anglaise 0593
- Asiatique 0305
- Canadienne (Anglaise) 0352
- Canadienne (Française) 0355
- Germanique 0311
- Latino-américaine 0312
- Moyen-orientale 0315
- Romane 0313
- Slave et est-européenne 0314

PHILOSOPHIE, RELIGION ET THÉOLOGIE
Philosophie 0422
Religion
- Généralités 0318
- Clergé 0319
- Études bibliques 0321
- Histoire des religions 0320
- Philosophie de la religion 0322

Théologie 0469

SCIENCES SOCIALES
Anthropologie
- Archéologie 0324
- Culturelle 0326
- Physique 0327

Droit 0398
Économie
- Généralités 0501
- Commerce-Affaires 0505
- Économie agricole 0503
- Économie du travail 0510
- Finances 0508
- Histoire 0509
- Théorie 0511

Études américaines 0323
Études canadiennes 0385
Études féministes 0453
Folklore 0358
Géographie 0366
Gérontologie 0351
Gestion des affaires
- Généralités 0310
- Administration 0454
- Banques 0770
- Comptabilité 0272
- Marketing 0338

Histoire
- Histoire générale 0578
- Ancienne 0579
- Médiévale 0581
- Moderne 0582
- Histoire des noirs 0328
- Africaine 0331
- Canadienne 0334
- États-Unis 0337
- Européenne 0335
- Moyen-orientale 0333
- Latino-américaine 0336
- Asie, Australie et Océanie 0332

Histoire des sciences 0585
Loisirs 0814
Planification urbaine et régionale 0999
Science politique
- Généralités 0615
- Administration publique 0617
- Droit et relations internationales 0616

Sociologie
- Généralités 0626
- Aide et bien-être social 0630
- Criminologie et établissements pénitentiaires 0627
- Démographie 0938
- Études de l' individu et de la famille 0628
- Études des relations interethniques et des relations raciales 0631
- Structure et développement social 0700
- Théorie et méthodes. 0344
- Travail et relations industrielles 0629

Transports 0709
Travail social 0452

SCIENCES ET INGÉNIERIE

SCIENCES BIOLOGIQUES
Agriculture
- Généralités 0473
- Agronomie. 0285
- Alimentation et technologie alimentaire 0359
- Culture 0479
- Élevage et alimentation 0475
- Exploitation des pâturages 0777
- Pathologie animale 0476
- Pathologie végétale 0480
- Physiologie végétale 0817
- Sylviculture et faune 0478
- Technologie du bois 0746

Biologie
- Généralités 0306
- Anatomie 0287
- Biologie (Statistiques) 0308
- Biologie moléculaire 0307
- Botanique 0309
- Cellule 0379
- Écologie 0329
- Entomologie 0353
- Génétique 0369
- Limnologie 0793
- Microbiologie 0410
- Neurologie 0317
- Océanographie 0416
- Physiologie 0433
- Radiation 0821
- Science vétérinaire 0778
- Zoologie 0472

Biophysique
- Généralités 0786
- Medicale 0760

SCIENCES DE LA TERRE
Biogéochimie 0425
Géochimie 0996
Géodésie 0370
Géographie physique 0368
Géologie 0372
Géophysique 0373
Hydrologie 0388
Minéralogie 0411
Océanographie physique 0415
Paléobotanique 0345
Paléoécologie 0426
Paléontologie 0418
Paléozoologie 0985
Palynologie 0427

SCIENCES DE LA SANTÉ ET DE L'ENVIRONNEMENT
Économie domestique 0386
Sciences de l'environnement 0768
Sciences de la santé
- Généralités 0566
- Administration des hôpitaux 0769
- Alimentation et nutrition 0570
- Audiologie 0300
- Chimiothérapie 0992
- Dentisterie 0567
- Développement humain 0758
- Enseignement 0350
- Immunologie 0982
- Loisirs 0575
- Médecine du travail et thérapie 0354
- Médecine et chirurgie 0564
- Obstétrique et gynécologie 0380
- Ophtalmologie 0381
- Orthophonie 0460
- Pathologie 0571
- Pharmacie 0572
- Pharmacologie 0419
- Physiothérapie 0382
- Radiologie 0574
- Santé mentale 0347
- Santé publique 0573
- Soins infirmiers 0569
- Toxicologie 0383

SCIENCES PHYSIQUES
Sciences Pures
Chimie
- Généralités 0485
- Biochimie 487
- Chimie agricole 0749
- Chimie analytique 0486
- Chimie minérale 0488
- Chimie nucléaire 0738
- Chimie organique 0490
- Chimie pharmaceutique 0491
- Physique 0494
- PolymÈres 0495
- Radiation 0754

Mathématiques 0405
Physique
- Généralités 0605
- Acoustique 0986
- Astronomie et astrophysique 0606
- Électronique et électricité 0607
- Fluides et plasma 0759
- Météorologie 0608
- Optique 0752
- Particules (Physique nucléaire) 0798
- Physique atomique 0748
- Physique de l'état solide 0611
- Physique moléculaire 0609
- Physique nucléaire 0610
- Radiation 0756

Statistiques 0463

Sciences Appliqués Et Technologie
Informatique 0984
Ingénierie
- Généralités 0537
- Agricole 0539
- Automobile 0540
- Biomédicale 0541
- Chaleur et thermodynamique 0348
- Conditionnement (Emballage) 0549
- Génie aérospatial 0538
- Génie chimique 0542
- Génie civil 0543
- Génie électronique et électrique 0544
- Génie industriel 0546
- Génie mécanique 0548
- Génie nucléaire 0552
- Ingénierie des systèmes 0790
- Mécanique navale 0547
- Métallurgie 0743
- Science des matériaux 0794
- Technique du pétrole 0765
- Technique minière 0551
- Techniques sanitaires et municipales 0554
- Technologie hydraulique 0545

Mécanique appliquée 0346
Géotechnologie 0428
Matières plastiques (Technologie) 0795
Recherche opérationnelle 0796
Textiles et tissus (Technologie) 0794

PSYCHOLOGIE
Généralités 0621
Personnalité 0625
Psychobiologie 0349
Psychologie clinique 0622
Psychologie du comportement 0384
Psychologie du développement 0620
Psychologie expérimentale 0623
Psychologie industrielle 0624
Psychologie physiologique 0989
Psychologie sociale 0451
Psychométrie 0632

IMMUNOHISTOCHEMICAL STUDY OF CONNEXIN43 AND ASTROCYTIC GAP JUNCTIONS IN NORMAL AND INJURED SPINAL CORD OF RAT

BY

UTA NICOLA FRANKENSTEIN

A Thesis submitted to the Faculty of Graduate Studies of the University of Manitoba in partial fulfillment of the requirements of the degree of

MASTER OF SCIENCE

TABLE OF CONTENTS

ACKNOWLEDGEMENTS

An array of people deserve and have my appreciation for their help throughout this program:

Dr. Nagy, if thesis co-authorship would be an option, you would definitely be on the cover of this book. Thanks for the many conversations about science, life, and life in science. I learned a lot from you and will never forget the two years I spent in your lab.

-Thanks to Rick Hansen, who wheeled 40,000 km around the world to raise funds for spinal cord research and rehabilitation. Support from the Rick Hansen Man in Motion Foundation enables scientists to test new ideas and technologies in spinal cord injury research and contribute to the quality of life of those in need.

-Thank you to my advisory committee, Drs. Cheng and Nance for the support during oral evaluation times and for reading my thesis. You were an excellent committee.

-Bernard Boguski, who was always there when I needed a helping hand and who taught me how to section, mount, coverslip, perfuse, make up solutions.....

-Andrew Ochalski and Mike Sawchuk, who taught me a lot about science and many other issues in life; the M-land times were a great initiation into student social life.

-Dr. Zahid Hossain, my "oral dictionary", thanks for answering all my questions.

-My fellow students, Bruce Lynn, Li Jian, Li Wei and Ni Lisa, thanks for the beer and cigarette sessions over which discussions about research have always been most fun and educational.

-Gerald Stelmack, who took the time to show me neat biochemical procedures.

-Richard, although you don't think you deserve a spot on this page, trust me, you did more than your part.

-Dr. Susan Kasper, I enjoyed your good german baking, your lectures and our conversations.

My studies in the Spinal Cord Research Center have been an invaluable experience, I have made many new friends, and the education I received here has not only broadened my understanding of science, but will always be a powerful tool in my future endeavours.

II. ABSTRACT

The immunolocalization and distribution patterns of the astrocytic gap junctional protein connexin43 (Cx43) were investigated in relation to temporal and spatial parameters of neuron loss, reactive gliosis and tissue damage in a trauma model of spinal cord injury (sci) induced by clip compression. At 1 and 3 days post-sci, Cx43 labelling in regions of severe neuron loss up to 0.5 mm adjacent to the compression site was, compared with that in normal spinal cord tissue, more sparse and more intense with both of two different sequence-specific anti-Cx43 antibodies utilized. At these survival times, grey matter areas of moderate to mild neuron depletion at distances of 0.5 to 1.5 mm from the compression site corresponded to those exhibiting a loss of immunolabelling with one of the anti-Cx43 antibodies. These regions of loss demarcated a zone separating intensified from normal staining and contained intensified labelling with another antibody suggesting that the loss with the former was due to masking of one of the Cx43 epitopes. By 7 days post-sci, Cx43 labelling was absent with both antibodies in all regions extending up to 1 mm from the lesion site. The distribution of astrocytes labelled for glial fibrillary protein (GFAP) in white and grey matter corresponded closely to that of Cx43 at 1 day, but less so at 3 days when they were evident at radial distances inward from the spinal cord periphery where Cx43 labelling was absent. By 7 days post-sci, Cx43 was colocalized with GFAP-positive astrocytes in a surviving outer rim of spinal cord tissue, which diminished in radial dimensions closer to the lesion site, and with astrocytic processes on blood vessels closest to the lesion. The results indicate that the phenomena of Cx43 epitope masking previously observed at excitotoxin lesions in brain also occurs after trauma-induced sci, that areas of neuronal loss and white matter damage predict fairly well those subject to alterations in Cx43 labelling, and that astrocytes during their transformation to a reactive form, at least in spinal cord, undergo a transition phase characterized by atypical Cx43 labelling possibly reflecting altered Cx43 localization or expression.

III. INTRODUCTION

III.1. Gap junctions

One of the most interesting cell junctions is the gap junction since it gives cells the ability to communicate with each other. Gap junctions are distributed throughout the peripheral (PNS) and central (CNS) nervous system. The first documentations of gap junctions were in the crayfish nerve cord (Fursphan et al., 1959) and Mauthner cells of the gold fish brain (Robertson et al., 1963). Thirty years later, gap junctions have been shown in virtually all tissues except striated muscle, erythrocytes and spermatozoa (Dermietzel et al., 1993). The communicative ability of cells via gap junctions has been demonstrated in studies of metabolic cooperation, electrical coupling and dye transfer.

Gap junctions are intercellular hemichannels (connexons) composed of six subunits or connexins (Makowski et al., 1977). When connexons of two cells allign, they form a continuous aqueous channel that allows the passage of small molecules and ions and thus couple cells metabolically and electrotonically (for review, see Bennett et al., 1991). These intercellular channels are about 1.5 nm in diameter and allow the passage of molecules no larger than 1,000-1,500 daltons. The channel excludes passage of macromolecules such as proteins or polysaccharides, but allows the passage of inorganic ions, amino acids, vitamins, low molecular weight trophic factors and other regulatory molecules (Loewenstein, 1981). Rapid opening or closure of gap junction channels is controlled by a process called gating. This process is influenced by a variety of factors including calcium, pH, phosphorylation of junctional proteins, transmembrane voltage, neurotransmitter, growth factors and steroids (Maldonado et al., 1988; Randriamampita et al., 1988; Saez et al., 1986; Spray and Bennett, 1985).

Thin section electron micrographs showed gap junctions as two adjacent cell membranes separated by a 2 nm space or "gap" (Revel et al., 1967). The hexagonal lattice of connexons in freeze fracture studies of gap junctions were seen as clusters of homogeneous intramembrane particles associated with the protoplasmic fracture face (P fracture face) and a complementary array of pits on the ectoplasmic fracture face (E fracture face) (Peracchia, 1980). Gap junction size may vary depending on the tissue examined. Gap junctions between rod and cone terminals are very small consisting of no more than 30-50 connexons (Bennett and Goodenough, 1978). Granulosa cell junctions may vary from an aggregation of 2 to 3 connexons to plaques of 2000 connexons covering approximately 35-40 μm^2 of plasma membrane (Larsen et al., 1981).

Gap junctions provide means of communication for excitable and non-excitable cells. In excitable cells, gap junctions provide a low resistance pathway for ion current passage to the coupled neighbouring cell (Hertzberg et al., 1981). In heart, gap junctions allow current flow from the sino-atrial node through the Purkinje system to ultimately lead to contraction of the ventricles (Weidmann, 1952). In the nervous system, the electrotonic gap junction permits more rapid synaptic transmission than a chemical synapse (Bennett, 1977). In non-excitable cells, gap junctional cell-cell communication is presumed to play a role in the transfer of signalling molecules and exchange of nutrients (Spray et al., 1985). Gap junctional coupling between non-excitable cells has been implicated in phenomena such as embryogenesis (Pitts, 1978), development (Wolpert, 1978) and growth (Loewenstein et al., 1978).

New insights into the study of gap junctions have been gained by the identification of subunit gap junctional proteins known as connexins (see below). The discovery of connexins has facilitated functional studies of gap junctions by allowing molecular analysis of

junctional properties and expression patterns under particular physiological or pathological conditions.

III.2. Connexins

Gap junctions are composed of six subunits of connexins. Connexins are transmembrane proteins that have four hydrophobic transmembrane spans and two extracellular domains. The extracellular domains are the most conserved regions whereas the transmembrane regions are somewhat less conserved (Beyer, 1993). To date, the connexin family is composed of approximately twelve members.

Using cDNAs coding for the rat liver 27 kDa molecule Paul (1986) identified the first connexin (Cx), a 32 kDa polypeptide named Cx32. Cx stands for the name of the protein family and a numeric index indicates the molecular mass in kilodaltons. Kumar and Gilula (1986) cloned a cDNA for its human counterpart. The amphibian homologue is xenopus Cx30 which shares 71% identical amino acids with the rat or human Cx32 (Gimlich et al., 1988). Screening a rat myocardial library with the Cx32 cDNA at reduced stringency enabled Beyer (1987) to identify a homologous polypeptide of 43kDa. This polypeptide was Cx43 and contained 43% identical amino acids to the protein cloned from rat liver. Zhang and Nicholson (1989) identified Cx26 in liver, which shared amino acid sequences with Cx32 and Cx43 over the length of the molecule (Beyer et al., 1990). Hoh et al. (1991) cloned Cx31 from rat genomic DNA and found it to be most abundantly expressed in placenta. Cx38 was cloned from a xenopus embryo library and is expressed in oocytes and early embryos (Ebihara et al., 1989). Cx42 and 45 were identified (Beyer, 1990) by screening a chick embryo cDNA library with a Cx43 probe. Cx42 and Cx45 are expressed in developing myocardium. MP70 is a 70 kDa lens protein that has not yet been cloned,

however, the N-terminus of MP70 shares the exact amino acid sequence of a 46 kDa polypeptide (Cx46) isolated from a rat lens cDNA library. The relationship of MP70 to Cx46 is still under investigation (Beyer et al., 1993). Cx56 was cloned by Rup and Beyer (1993) and is expressed in chick lens. Genomic cloning and polymerase chain reaction have led to the identification of further expressed connexins, including Cx31.1, Cx33 and Cx37 and have increased the number of known mammalian connexins to about a dozen (Haeflinger et al., 1992; Willecke et al., 1990). All connexin family members possess a similar gene structure, exhibit about 50% sequence homology at the amino acid level and show diverse patterns of tissue expression.

III.3. Neuronal gap junctions in CNS

It is well accepted that gap junctions mediate intercellular electrotonic and metabolic coupling between neurons, macroglia and various other cell types in the CNS (for reviews see Bennett and Goodenough, 1978; Loewenstein, 1981, Sotelo and Korn, 1978; Beyer, 1993). A large body of evidence suggests that electrotonic transmission between particular assemblies of neurons constitutes an important mode of intercellular communication. Even though gap junctions between neurons were first demonstrated in the CNS of lower vertebrates several decades ago (Fursphan and Potter, 1959), the extent of their occurrence and the nature of their contribution to interneuronal communication in mammalian neuronal systems are still largely matters of speculation. Evidence for the existence of gap junctions between mammalian CNS neurons has been obtained from conventional and freeze fracture electron microscopy, intracellular recordings from coupled cells *in vitro* and dye coupling via cell-to-cell diffusion of tracer. Several studies have provided support for the proposition that gap junctions make a significant contribution to interneuronal communication. Llinas

(1985) demonstrated that gap junctions between neurons are involved in mediating synchrony among active cells and presented evidence that such synchronous activity of inferior olive neurons was determined by the dynamic state of electrical coupling between these cells. Further, he suggested that the organization of cells into synchronous active clusters may be achieved by a process involving selective uncoupling of sets of neurons (Llinas and Yarom, 1991). Synchronous activity has also been demonstrated between magnocellar neurons of the supraoptic and paraventricular nuclei (Belin and Moos, 1986; Yang and Hatton, 1988). In females, dye-coupling between these neurons depended on the physiological state of the animal and was found to be higher in the lactating or maternally behaving female. Interestingly, although there was an intermingled distribution of vasopressin- and oxytocin- containing cell bodies, dye-transfer occurred only between cells containing the same peptide. On the basis of these results, it has been suggested that electrotonic coupling in the case of oxytocin cells may serve to coordinate activation during the periodic high frequency bursts of action potentials that they exhibit in response to suckling and thereby cause sufficient oxytocin release to evoke milk ejection (Hatton and Yang, 1990).

III.4. Astrocytic gap junctions in CNS

Ultrastructural, dye-transfer, and electrophysiological studies (Connors et al., 1984; Fischer and Kettenmann, 1985; Gutnick et al., 1981; Kettenmann et al., 1983; Kettenmann and Ransom, 1988; Schwartzkroin and Prince, 1979; Sipe and Moore, 1976; Waxman and Black, 1984) have provided strong support for the view that astrocytes are extensively coupled in vast networks to form what are defined as "functional syncytia" (Massa and Mugnaini, 1982; Mugnaini, 1986). Several reports indicate that gap junctions are

particularly numerous between astrocytic processes that ensheath chemical synapses, glomeruli and nodes of Ranvier, as well as between those at brain and vascular surfaces (Sipe and Moore, 1976; Waxman and Black, 1984; Mugnaini, 1986). While these reports suggest that astrocytic gap junctions are ubiquitous in the CNS, the functional significance of the observed local heterogeneities has remained largely unclear due to lack of knowledge of the global organization of gap junctions in the astrocytic syncytial network. Although many investigators have focused on the functions of astrocytes in normal and injured CNS (Walz, 1989), many questions still remain unanswered. One well-known role of astrocytes is to form structural barriers at vascular surfaces and to ensheath neuronal elements, thereby separating regions of dissimilar or fluctuating ionic composition and physically or metabolically compartmentalizing various neuronal components of the CNS. Astrocytes also contribute to extracellular potassium homeostasis by a process called spatial buffering (Walz, 1989). This involves the cell-to-cell redistribution of excess extracellular potassium through the cytoplasm of vast networks of contiguous astrocytes coupled by gap junctions (Bennett and Goodenough, 1978; Massa and Mugnaini, 1982; Walz, 1989).

III.5. Connexins in CNS

To date, 6 connexins have been detected in adult and developing CNS by blotting techniques. These include Cx26, Cx31, Cx32, Cx37, Cx43 and Cx45 in rat brain (Naus et al., 1990; Dupont et al., 1991; el Aoumari et al., 1990; Willecke et al., 1991). The cellular localization of these connexins is uncertain with the exception of Cx43 which is found in astrocytes. By Northern and Western blot analyses, Cx32 protein and mRNA appear during the second postnatal (P) week in developing brain, whereas Cx43 is detectable at embryonic (E) day 18 and increases or remains at relatively constant levels during development

(Belliveau et al., 1991). In the striatum of rats, the levels of Cx26 were reported to be high at E18 after which it decreased dramatically by P6, whereas Cx32 gradually increased from P14 to adulthood (Dermietzel et al., 1989). By ISHH, Cx32 mRNA was detected in the somata of neurons, glial cells and ependymal cells in various regions of 2 day old rat brain (Matsumoto et al., 1991).

In adult brain, Dermietzel (1989) suggested that some neurons express Cx32 on the basis of their finding that 20% of the cells in basal ganglia, thalamus and brainstem that were immunopositive for Cx32 were also positive for neuron specific enolase. Neurons elsewhere in brain were devoid of Cx32. Extensive immunohistochemical analyses have been conducted in brain using an antibody (designated A893) against Cx32 (Nagy et al., 1988; Yamamoto et al., 1989). This antibody labelled neuronal gap junctions, glial gap junctions and a class of varicose axons whose identity has not yet been determined. Therefore, the former observation is consistent with the finding by Dermietzel et al. (1989) in that some neurons express Cx32 or a similar connexin. In separate LM and EM work, Cx43-immunoreactive neuronal gap junctions were never observed (Yamamoto et al., 1990, 1991). Micevych and Abelson (1991) reported autoradiographic labelling for Cx32 mRNA in what appeared to be neurons in the midlayers of the cerebral cortex, islands of Calleja, pyramidal and granule cells of the hippocampus and lateral habenula of rat brain.

On the basis of immunohistochemical, Western blot and Northern blot analyses of neuronal and glial cultures, it was reported by some that astrocytes express Cx43 protein and mRNA and contain no detectable levels of Cx32 mRNA (Finch and Paul, 1989; Dermietzel et al., 1991; Giaume et al., 1991; Naus et al., 1991). In brain, Dermietzel et al. (1989) reported that only astrocytes were immunopositive for Cx43. Yamamoto et al. (1990b, 1991) have shown that astrocytic gap junctions in rat are immunolabelled with

antibodies against Cx43 and extensive work with these antibodies indicates that the majority of astrocytes express Cx43. However, dye-coupling between cultured astrocytes was shown to be reduced by microinjection of a polyclonal antibody against Cx32 (Dudek et al., 1988). On the basis of these results, it seems possible that a subpopulation of astrocytes, in addition to expressing Cx43, may express a protein closely related to Cx32. While Cx43-immunopositive gap junctions were occasionally observed between oligodendrocytes and astrocytes (Nagy and Yamamoto, unpublished observations), the cytoplasmic membrane of the oligodendrocyte was seldom labelled. These junctions were thus asymmetrically stained suggesting heterologous coupling between connexins. Heterologous junctions have also been reported *in vitro* by freeze fracturing of co-cultures (Massa and Mugnaini, 1982), and recent electrophysiological evidence for such chimeric junctions was provided by Ransom and Kettenmann (1990).

III.6. Distribution of connexin43 in brain

In light microscope (LM) immunolocalization studies of connexins in sections of CNS tissue, fluorescence or peroxidase immunoreactivity often consists of small spots or aggregations of puncta. Electron microscope (EM) immunohistochemical studies have shown that Cx43 immunoreactivity (Cx43-IR) is associated with what can be clearly identified morphologically as astrocytic gap junctions (Yamamoto et al., 1990b, 1991) and this has been confirmed by immunogold localization methods (Dermietzel et al., 1989; Miragall et al., 1992; Nagy and Yamamoto, unpublished observations). Relatively greater numbers of labelled gap junctions were found around neuronal elements such as those between astrocytic processes surrounding dendrites and synaptic glomeruli. With respect to the distribution of Cx43 within cells, Cx43 was detected only at or near the vicinity of

found to be unlabelled for Cx43. As noted above, virtually all labelling was punctate in nature. From correlative examination of LM and EM micrographs, it appears that the vast majority of puncta seen by LM correspond to individual or clusters of labelled gap junctions identified by EM. Based on the density and complexity of Cx43 labelling observed and apart from clues provided by its ubiquity, it has been noted (Yamamoto et al., 1990a) that were it not for extensive EM analysis, it would be very difficult to definitively identify the cell type responsible for the Cx43 immunolabelling obtained by LM.

It has been found that Cx43 is widely distributed in rat brain, which is not surprising given the apparent ubiquitous distribution of astrocytic gap junctions in the CNS. Moreover the density of Cx43-IR was highly uneven among brain regions (Yamamoto et al., 1990a). This suggested a considerable heterogeneity of astrocytic gap junctions as reflected by the numbers of Cx43-immunoreactive puncta in individual brain areas (Yamamoto et al., 1990a). It has been confirmed that the relative levels of Cx43, as detected on Western blots, vary widely among brain areas and comparisons of these levels with the densities of Cx43-IR observed in the same areas of tissue sections processed immunohistochemically for Cx43 yields a strong positive correlation (Nagy et al., 1992). Thus, the striking regional heterogeneity in immunoreactivity can be attributed to differences in the amounts of Cx43 expressed. By *in vitro* approaches, it was shown that astrocytes from different brain regions of neonatal rat exhibit markedly different levels of Cx43 and degrees of dye-coupling after they have been grown to confluence (Batter et al., 1992).

III.7. Astrocytic connexin43 expression after CNS injury

Damage to CNS results in the transformation of normal astrocytes to reactive astrocytes, a phenomenon known as reactive astrogliosis. Whether these changes are

beneficial or detrimental to CNS reparative processes remains a controversial issue (Eddelston and Mucke, 1993). In response to CNS trauma the astrocytic syncytial network is presumably reorganized to accommodate environmental local changes in ion concentrations. One process thought to be critical for the maintenance of a normal metabolic environment around neurons is astrocytic spatial buffering. Cx43, a key component of gap junctional coupling between astrocytes responds to the presumably unusual spatial buffering demands required after CNS trauma and subsequent neuronal degeneration and death. For example, increases in Cx43-IR in the facial motor nucleus have been observed as early as 45 min after lesions of the facial motor nerve (Rohlman et al., 1994). Vukelic et al. (1991) demonstrated that kainic acid (KA) injections into the thalamus led to neuron depletion and elimination of antibody recognition of Cx43 in immunohistochemically processed tissue. This response was further investigated by Western blot and ultrastructural analyses (Hossain et al., 1994a) using different sequence-specific antibodies to Cx43. Immunohistochemical analyses of KA-injected thalamus, striatum and hippocampus with one antibody designated 18A-8 (against amino acids 346-363) showed that Cx43-IR was increased 5 h after KA injections, absent by 24 h, and for up to two weeks post-injection and began to return to less than normal levels by 2-3 weeks post-injection. Analyses of KA lesions with other sequence-specific antibodies (16A-8, an antibody against amino acids 241-260 of the Cx43 sequence) revealed not only the presence of Cx43, but in some instances an increase in labelling after 1 week survival time. By Western blot analyses, homogenates of KA-injected striatum contained Cx43 levels that were near normal or even slightly increased at various survival times (Hossain et al., 1994a). EM investigations of thalamus at 1 week survival time revealed a general absence of gap junctions within KA lesion sites. Thus, the authors suggest that the loss of immunohistochemically detectable Cx43 at KA lesion sites with

antibody 18A-8 depends on the functional state of astrocytes and Cx43 may undergo a molecular transformation such that epitopes recognized by antibody in one state are hidden in another and those ordinarily hidden become exposed. The absence of gap junctions at the ultrastructural level suggests that Cx43 may be located at some other cellular site than gap junctional plaques. To investigate this possibility, Ochalski et al. (1995) looked at the fate of Cx43-IR at various survival times after thalamic KA and striatal NMDA lesions. At the ultrastructural level, the authors demonstrated that Cx43-IR with 18A-8 and 16A-8 was restricted to astrocytic gap junctions in normal tissue, increased with 18A-8 at 6 h post-lesion and was absent at 24 h. In contrast to the absence of staining with antibody 18A-8 at 24 h, 16A-8 immunoreactivity included gap junctional, annular profile and non-junctional membrane labelling. At 2-3 days survival time, 16A-8 continued to label these structures as well as astrocytic cytoplasm, annular profiles present in astrocytes and multivesicular clusters. At later survival times, 16A-8 staining was seen almost exclusively in multivesicular clusters. The authors suggest that these clusters may arise from astrocytic autophagy. In NMDA lesioned tissue, ultrastructural disruption and gap junction disassembly progressed more slowly and Cx43-IR as detected by 18A-8 and 16A-8 persisted at decreased levels.

In studies of global forebrain ischemia, Hossain et al. (1994c) demonstrated that Cx43 increases following mild or moderate insult, but decreases in severely affected regions as evidenced by degrees of neuron loss. Areas of Cx43-IR increase were similar to those at the periphery of NMDA lesions (Ochalski et al., 1995) where Cx43 was concentrated in astrocytic processes and their gap junctions. Areas of Cx43 loss resembled kainic acid and NMDA lesions where astrocytic gap junctions were absent or reduced.

III.8. Rationale for the present studies

Elimination of gap junctions and Cx43 immunolabelling may parallel neuron loss and reflect dependence of Cx43 expression on astrocyte-neuron interactions. If Cx43 expression and astrocytic junctional communication are under stringent control, then more complicated events likely underlie the above described results. For example, elevated Cx43 in ischemic striatal regions exhibiting limited neuronal damage may indicate an enhanced coupling state of astrocytes in an attempt to support neuronal survival. Conversely, decreased Cx43 in striatal regions with severe neuronal damage suggests reduced junctional coupling and an attempt by astrocytes to sever communication with their neighbors thereby restricting the outward flow of potentially damaging metabolites. We hypothesize that if such an attempt to limit damage by closure or elimination of gap junctions is characteristic of astrocytes, as proposed for other cells (Dermietzel et al., 1987; Yee and Revel, 1978), and is evoked to excess, this might compromise astrocytic spatial buffering and contribute secondarily to, rather than limit, neuronal damage. For example, damage could cause astrocytic uncoupling in undesirably large areas of tissue leading to failure of spatial buffering, build-up of extracellular K^+ and neuronal injury or death. Although literature on astrocytic gap junctional reorganization after various types of CNS lesions is vast, no one has used the spinal cord compression model to investigate gap junctional Cx43 in response to such an insult. Injury to the spinal cord results in a cascade of events including astrogliosis, the invasion of inflammatory cells and the formation of cavities or glial scars. The astrocytic response occurs at the lesion site in close vicinity to neural tissue affected by the primary lesion. Thus, we thought to determine the response of astrocytic gap junctions to spinal cord injuries as deduced from analysis of Cx43 expression, antibody recognition and gap junction localization. We used the clip compression injury model since it closely resembles human

cord injuries (Tator, 1991) and since the force and duration of clip closure/cord compression can be precisely calibrated to obtain quantifiable and reproducible injuries (Theriault and Tator, 1994).

IV. MATERIAL AND METHODS

IV.1. Antibodies

Two rabbit polyclonal anti-Cx43 antibodies utilized were generated against BSA-conjugated peptides corresponding to amino acids 346-363 or 241-260 of the Cx43 sequence and designated 18A-8 and 16A-8, respectively. These antibodies have been extensively used in our laboratory and their specificity has been well established by Western blots of brain and heart homogenates. In Western blots of brain, 18A-8 binds a 43 kDa double band and a single band with a mol. wt. of 41 kDa. The 43 kDa protein corresponds to the phosphorylated form of Cx43 which migrates more slowly than the unphosphorylated 41 kDa protein (Hossain et al., 1994a). In Western blots of heart, which contains very little of the 41 kDa form, 18A-8 binds the phosphorylated 43kDa form (Yamamoto et al., 1990b). By light microscopy (LM), both antibodies produce similar punctate labelling of gap junctions in sections of heart and brain (Yamamoto et al., 1990b). By electron microscopy (EM), immunoreactivity was localized to glial gap junctions and intracellularly within glial processes at sites near these junctions (Yamamoto et al., 1990b, Hossain et al., 1994a). The specificity of both antibodies was also indicated by elimination of all staining by preabsorption of antibody 18A-8 (Hossain et al., 1994c) and 16A-8 (Hossain et al., 1994a) with peptides against which they were raised. In the present experiments, no immunoreactivity was observed in sections processed after omission of the primary antibody.

A mouse monoclonal antibody against glial fibrillary acidic protein (GFAP) (Boehringer Mannheim) was applied to identify astrocytes. Additional anti-GFAP antibodies tested included: a preparation of mixed monoclonal antibody cocktail (Sternberger Monoclonals Inc.) composed of three monoclonal antibodies to GFAP derived from the Bigner-Eng

clones MAb1B4, MAb2E1 and Mab11 as well as monoclonal anti-GFAP from the Sternberger clone SMI21; a mouse monoclonal anti-astrocyte antibody (Swant 325); and a polyclonal rabbit anti-GFAP antibody generously provided by Dr. Lawrence F. Eng (Pathology Research, Stanford University School of Medicine).

For the peroxidase anti-peroxidase (PAP) method, the secondary antibody used was goat anti-rabbit IgG (since the primary antiserum was raised in rabbit) purchased from Sternberger Monoclonals Inc., Baltimore, MD. Secondary antibodies for double immunofluorescence included a Cy3-conjugated sheep anti-rabbit antibody from Sigma Immunochemicals and a fluorescein isothiocyanate (FITC)-conjugated horse anti-mouse antibody obtained from Dimension Labs. The secondary antibody used in the ethidium bromide (EB) (Sigma Immunochemicals) counterstaining protocol was an FITC-conjugated donkey anti-rabbit antibody obtained from Amersham. EB is a red fluorescent dye that specifically binds to nucleic acids (LePeq, 1971). The third antibody in the PAP method was rabbit PAP from Sternberger Monoclonals Inc..

IV.2. Animals and surgical procedures

A total of 30 female Wistar rats weighing 200-250 g were used in the present study. Eight female Wistar rats were used to examine Cx43 in normal spinal cord, and groups of 6 to 8 animals were examined at survival times of 1, 3 and 7 days after spinal cord compression injury.

The spinal cord compression injury in the present study was performed by Dr. Elizabeth Theriault (Playfair Neuroscience Unit, University of Toronto) as previously described (Theriault and Tator, 1994). All animals were anesthetized using 2% halothane and oxide/oxygen (2:1) inhalation. Fenicol (1% chloramphenicol, Alcon Canada) was applied to

the eyes of the animals to avoid corneal abrasions. Body temperature was monitored by a rectal probe. Prior to a dorsal midline incision from the superior nuchal line to the upper thoracic region, the back and neck of each animal was shaven and prepared with 70% alcohol and betadine. To expose the spinal cord at C7-T2, the muscular layers overlying the cord were separated. Muscle and fascia were removed from the facets and pedicles of the vertebrae to allow for a full lateral exposure of the cord. The vertebrae were cleared of laminae and facets with malleus nippers without exerting pressure on the spinal cord. A modified Kerr-Lougheed aneurysm clip with a closing force of 35 g was used to produce a standardized compression injury of the cervical spinal cord at C8-T1. The clip was placed extradurally around the C8-T1 spinal cord, one blade of the clip being placed anteriorly, the other posteriorly. The cord was then compressed for one minute and the clip was removed. The surgical site was closed in layers with sutures. After surgery, animals were treated with 5 ml dextrose/saline for volume repletion and recovered on heated water pads (37 °C). Animals with a punctured dura were excluded from the study. To ensure consistency of the injury, only one person performed the surgery (E. T.) and time under anesthesia, position, release, and removal of the clip were standardized. Spinal cord injured animals received manual bladder eliminations three times daily throughout the survival period. All animals were individually housed at a 12 h light/dark cycle and had free access to food and water.

IV.3. Tissue Preparation

All animals were deeply anesthetized with equithesin and transcardially perfused on ice. The thoracic cavity and diaphragm were opened to expose the heart. The left ventricle was pierced by a 23 gage needle attached to the tubing of the perfusion pump. The right atrium was then cut to allow blood and perfusion fluid outflow. Perfusion rate was kept

constant at 40 ml/min. Prefixative solution consisted of 70 ml of cold (4 °C) 50 mM sodium phosphate buffer (PB) containing 0.9% saline, 0.1% sodium nitrite, and heparin (1unit/ml) adjusted to pH 7.4 per rat. The fixative solution consisted of 400 ml of 0.1 M PB containing 4% paraformaldehyde adjusted to pH 7.4 per rat. The spinal cords were freed of the dura matter, removed and post-fixed for 2 h in 10 ml of the fixative solution. For cryoprotection, a 3 mm spinal cord block of 1.5 mm at each side of the lesion epicenter was transferred to 10 ml of 50 mM PB containing 15% sucrose (pH 7.4) for subsequent sectioning on the cryostat, while the remainder of the rostral spinal cord was segmented into three further 3 mm blocks (1.5-3.5 mm, 4.5-7.5 mm and 7.5-10.5 mm from the lesion epicenter) and transferred to 10 ml of 50 mM PB containing 25% sucrose and 10% glycerol (pH 7.4) for sectioning on the sliding microtome. Spinal cords were stored in sucrose solutions for a minimum of 4 days and transferred to fresh sucrose solutions at least two times to allow for optimal cryoprotection of the tissue.

IV.3. Immunohistochemistry

Frozen sections were cut transverse or parasagittal at a thickness of 20 μm. The 3 mm block containing the spinal cord crush epicenter was sectioned on a cryostat and collected on gelatinized slides, while all remaining tissue was sectioned on a sliding microtome and collected free-floating in PB containing 0.9% saline (PBS). Sections on slides were washed for 1 h at room temperature in 0.1 M PBS containing 0.3% Triton X-100 (PBST) while free-floating sections were washed overnight in PBST prior to processing. Sections were processed by the PAP method, double immunofluorescence, or counterstained with ethidium bromide or cresyl violet as described below. All antibodies and immunoreagents were

diluted in PBST. Primary incubations were carried out at 4 °C for 48-72 h and incubations with secondary immunoreagents and washes were carried out at room temperature.

IV.4.1. *Peroxidase anti-peroxidase (PAP) method.* Primary antibodies were used at the following dilutions: the rabbit anti-Cx43 antibody 18A-8, 1:2000; rabbit anti-Cx43 antibody 16A-8, 1:1000; mouse monoclonal anti-GFAP, 1:25. To eliminate endogenous peroxidase activity, spinal cord crush epicenter sections were incubated in 0.1 M phosphate buffer containing 0.2% H2O2 for 30 min prior to antibody application. After primary incubation with 18A-8, free-floating sections as well as sections mounted on slides were processed by the PAP method and first washed for 1 h and then incubated for 1.5 h with goat anti-rabbit IgG diluted 1:100. After a further 1 h wash sections were incubated with rabbit PAP diluted 1:500. The final washes consisted of one 10 min wash in PBST followed by two 10 min washes in 50 mM Tris-HCl buffer, pH 7.4. The sections were reacted in Tris-HCl buffer containing 0.02% 3,3-diaminobenzidine (DAB) and 0.005% hydrogen peroxide. Finally, sections were washed in Tris-HCl buffer, mounted onto slides from gelatin-alcohol, dehydrated in alcohol and coverslipped with Lipshaw mounting medium. Processing of spinal cord sections for antibody 16A-8 was carried out similarly as described above.

IV.4.2. *Immunofluorescence*. Slides mounted as well as free-floating sections processed for double immunofluoresence were simultaneously incubated with either anti-Cx43 (18A-8) diluted 1:2000 and anti-GFAP diluted 1:25 or with anti-Cx43 (16A-8) diluted 1:1000 and anti-GFAP diluted 1:25. Sections were then washed for 1 h and simultaneously incubated for 1.5 h with Cy3-conjugated sheep anti-rabbit antibody diluted 1:250 and FITC-conjugated horse anti-mouse antibody diluted 1:50. After a final wash (one 10 min wash in PBST and two 10 min washes in 50 mM Tris-HCl buffer, pH 7.4), slides were air-dried and coverslipped with anti-fade medium (Lennette, 1977; Valnes and Brandtzaeg, 1985),

whereas free-floating sections were mounted onto slides from 50 mM Tris-HCl buffer, pH 7.4, air-dried and then coverslipped.

IV.4.3. *Counterstaining.* Prior to counterstaining with EB, sections were incubated with the primary antibody 18A-8 as described above, followed by FITC-conjugated donkey anti-rabbit antibody. After a 30 min wash in PBS, counterstaining with EB was conducted in PBS for 2 to 5 min. at a concentration of 0.00005%. The slides were then briefly washed in PBS, air-dried and coverslipped with anti-fade medium (Schmued et al., 1982 and Franklin et al., 1981). At this concentration, EB produces a moderately bright Nissl stain of neuronal cytoplasm, nucleoli, and glial nuclei (Schmued et al., 1982). Several sections were also stained for Nissl substance with cresyl violet. Sections mounted onto slides were first rehydrated for 30 min in 50 mM PBS, counterstained in 0.05% cresyl violet for 5 min, then dehydrated in ascending levels of alcohol and cleared in Histoclear. Finally sections were coverslipped with Lipshaw mounting medium.

Sections were viewed with a Leitz Dialux 20 microscope equipped with Ploempak filter cubes L3 (excitation 450-490 nm; band pass 500-550 nm) and N2 (excitation 530-560 nm; long pass 580 nm) for FITC and for Cy3 fluorescence or ethidium bromide, respectively.

V. RESULTS

V.1. General observations

To optimize detection of Cx43 in sections taken for examination by LM, two fixation protocols were tested. The pH change protocol was previously shown to produce the optimal fixation procedure for Cx43 in brain (Yamamoto et al., 1990a,b, 1992; Nagy et al., 1992, Hossain et al., 1994a,c). In spinal cord, however, this fixation procedure generally resulted in less intense Cx43-IR throughout the spinal cord than seen with a weaker fixation procedure involving the use of 4% paraformaldehyde at neutral pH as described in the Methods section. Thus, the latter was used in all the present studies. Similarly, GFAP-immunopositive astrocytes were more intensely labelled in grey and white matter and specifically at grey/white matter borders with the neutral pH-4% paraformaldehyde fixation compared with the pH change fixation.

LM immunohistochemical staining patterns with anti-Cx43 18A-8 and 16A-8 antibody were virtually identical in grey and white matter of normal rat spinal cord. The only distinction was that 18A-8 produced a greater density of DAB immunoreaction product as previously observed in brain (Hossain et al., 1994a; Ochalski et al., 1995). Control staining with omission of the 18A-8, 16A-8 and GFAP antibodies showed no immunoreactivity in the spinal cord sections. The specificity of the antibodies has been described in the Methods section.

The overall distribution of Cx43 in the rat spinal cord was somewhat heterogeneous. Cx43-immunoreactive elements were therefore analyzed in spinal cord grey matter, which is typically divided into dorsal and ventral horn and more specifically into Rexed laminae I-X, and spinal cord white matter which is subdivided into dorsal column, lateral and ventral

funiculi. Cx43-IR exhibited three morphologically distinct patterns: 1) Many fine immunopositive puncta that were distributed throughout grey and white matter. These puncta were either round or oval shaped and varied in size depending on the area of the spinal cord examined. Otherwise they had a relatively uniform range of features and will be referred to simply as puncta. 2) Immunoreactive fine fibers in white matter which had puncta distributed along their length. Similar fibers were not observed in grey matter. 3) Annular patterns of continuous labelling or circular arrays of puncta enclosing an area devoid of staining. These annular profiles, previously described in brain (Yamamoto et al., 1990a), were observed throughout grey matter regions, but were more prominent in some areas.

V.2. Connexin43 in normal rat spinal cord

A general overview of Cx43 distribution in the C8-T1 region of the spinal cord is demonstrated in micrographs of transverse and parasagittal sections (Figs. 1A-G). Cx43 immunostaining was highly prominent in grey matter but, was also sparsely distributed throughout white matter (Fig. 1A). In transverse sections, intense Cx43-IR was observed in Rexed laminae I, lamina II (substantia gelatinosa) (Fig. 1B) and X (area surrounding central canal) (Figs. 1A and F). Rexed lamina X contained Cx43 puncta extending dorsally and enveloping the dorsal column (Fig. 1A). Thus, the most ventral aspect of the dorsal column was surrounded by intense Cx43 puncta in the grey matter. Fine Cx43 puncta were seen along fibers extending medially from lamina X into the dorsal column white matter and towards the medial septum (not shown).

The intense staining in the substantia gelatinosa was different from the generally fine punctate labelling observed in the majority of the spinal cord grey matter in that it consisted of many Cx43-immunoreactive annular profiles (Fig. 1B). These were of different sizes

ranging from 1 to 8 μm in diameter. This type of Cx43-IR has been previously described in the medial habenula of rat brain (Yamamoto et al., 1990a). Annular profiles were also observed in other regions of the grey matter, but were far more concentrated in the substantia gelatinosa. In sagittal sections of Lissauer's tract, many fine Cx43 puncta were seen along fibers running rostro-caudally within the tract (Fig. 1C). The majority of Cx43-immunoreactive elements, with the exception of the substantia gelatinosa, was fine and punctate as shown in Fig. 1D which provides an example of these fine puncta in the intermediate laminae of the spinal cord.

In the ventral horn, Cx43-immunopositive puncta were more intense within motor nuclei (Fig. 1E) and staining density was much higher around neuronal cell bodies, particularly motoneurons. Immunostaining in the vicinity of motoneurons consisted of finely dispersed Cx43-immunopositive puncta and some annular profile staining. Cx43-immunoreactive puncta were also seen among ependymal cells of the central canal (Fig. 1F) similar to the distribution of Cx43 in the ependymal layer of the ventricles in brain where staining by EM was demonstrated to be associated with gap junctions between ependymal cells and between the basal portion of these cells and glial processes (Yamamoto et al., 1990a). Intense Cx43 staining was observed along blood vessels throughout grey and white matter. Blood vessels radiating from white matter inwards toward grey matter were heavily laden with Cx43-immunoreactive puncta (Fig. 1G).

Cx43 was observed in all regions of white matter (Fig. 2). Cx43-immunoreactive puncta of various sizes and staining intensity were seen intercalated between myelineated fibers in white matter (Fig. 2A), along astrocytic processes (Fig. 2B), and within the glial limitans (Fig. 2C), as well as in the dorsal column and along individual fine processes of presumably astrocytes in the ventral and lateral white matter (Figs. 2D and E).

Bundles of myelinated fibers emanating from the ventral horn or entering the dorsal horn and dorsal column via the dorsal and lateral white matter were densely associated with Cx43 immunoreactive puncta (Fig. 2A). At various distances beyond the grey/white matter border, these fibers exhibited diminished levels of Cx43 staining as they radiated towards the periphery of the cord and was especially reduced after the fibers have travelled about two thirds of the distance from the grey/white matter border towards the cord surface.

In the most dorsal region of the dorsal column, Cx43 immunostaining had a honeycomb appearance (not shown) forming a mesh-like network close to the glial limitans. Similarly, Cx43-IR was previously seen associated with the cortical surface (Yamamato et al., 1990a) and blood vessels in cerebral cortex (Yamamoto et al., 1990b). Honeycomb staining was also observed in the lateral (Figs. 2B and C) and ventral funiculi where it was again most prominent in close proximity to the glial limitans. Ventrally in the dorsal column towards the central grey matter, Cx43 had a more fibrous appearance running dorsoventrally towards the central grey matter.

The entire periphery of the spinal cord white matter contained radial astrocytes which sent their processes towards the interior of the cord and extended thick processes to form the glial limitans. Fig. 2B shows Cx43 along astrocytes extending their endfeet to form the glial limitans. Cx43-immunopositive puncta of varying sizes and staining intensity are shown along these processes and distributed within the glial limitans in Fig. 2C.

V.3. Connexin43 in relation to neurons in normal spinal cord

Neuronal perikarya have been distinguished by size and density in Rexed laminae I-X of grey matter and were characterized as large, medium or small cell bodies, as previously described by Rhetelyi (1987). In normal cord, large motoneurons are found in the ventral

horn, whereas medium and small neurons are ubiquitously distributed throughout the spinal cord grey matter. In the dorsal horn, Rexed laminae I, II, and III are particularly apparent since they contain smaller and more densely packed cells, especially in the substantia gelatinosa, than any other laminae of the spinal cord. Some medium-sized neurons are also scattered throughout these laminae. In comparison to the more dorsal laminae, lamina IV is characterized by a lower density of neurons and the presence of several large neuronal cell bodies. Intermediate Rexed laminae V-VII contain many large neuronal somata and fewer numbers of medium and small neurons. Laminae V and VI constitute the ventral third of the dorsal horn and, together with lamina VII, contain a polymorphous cell population of small, medium and large neurons. Neurons in the ventral horn are arranged in groups rather than laminae as in the case of the dorsal horn. Thus, based on their location, groups of neurons intermingled with small and medium sized neurons in Rexed laminae VIII and IV can be identified as motoneurons. The area around the central canal or Rexed lamina X contains mainly neurons of medium size.

To compare Cx43 with neuronal staining in grey matter, sections were processed for 18A-8 and counterstained with ethidium bromide. Intense Cx43-IR and numerous annular profiles were seen in close proximity or surrounding neurons in Rexed laminae I and II. Ventrally in laminae III-VII, intensely stained Cx43 puncta were observed around small, medium, and large neurons and were also ubiquitously distributed throughout these laminae. In Rexed lamina X, intensely labelled fine Cx43-positive puncta again enveloped neurons and were seen throughout this area. The ventral horn, including areas in laminae VII, VIII and IX, also contained Cx43-immunopositive puncta around neuronal soma and intense punctate staining surrounding motoneurons. Fine puncta throughout the spinal cord grey

matter were seen in areas surrounding these neuronal soma, axons and blood vessels and annular profiles were often seen in the vicinity of neurons.

V.4. Neuron loss after compression injury

As seen in Nissl stained sections, tissue deterioration was most evident at the crush site in sections through the lesion epicenter. Further away from the crush site, degeneration was progressively less and became restricted first to both the ventral part of the dorsal column and the central canal area. Still further away the disintegration of tissue was even more restricted particularly to the ventral part of the dorsal column. At 1 day survival, Nissl stained transverse sections showed a total loss of neurons within the crush site, which was primarily characterized by tissue necrosis. Immediately adjacent to the crush site (Fig. 3A), neuron loss extended from the superficial tip of the dorsal horn to the ventral tip of the ventral horn. In some animals, many neurons were observed in lamina I and II, the most medial aspect of lamina III, and in the medioventral aspect of the ventral horn, which appeared to be spared from the insult. The remaining laminae (III-X) were devoid of neurons. The area around the central canal (Rexed lamina X) was often necrotic and devoid of neurons (not shown). This area of necrosis extended outward dorsoventrally and mediolaterally encompassing surrounding areas. At 0.5-1 mm rostral and caudal from the crush site, neuron loss was progressively less (Fig. 3B). More neurons were observed in the superficial dorsal and ventral horn areas such that Rexed laminae I-IV had a normal appearance of small and densely packed cells intermixed with a few scattered neurons of medium size, and ventral horn regions appeared relatively normal or contained neurons surrounded by necrotic tissue. Areas most usually affected by the injury were laminae V-VII where severe neuron loss was evident. However, in comparison to the crush site, some small

sized neurons were seen scattered within these areas. In sections furthest away from the crush site (1-1.5 mm rostral and caudal), neuron loss was restricted to patches in dorsal, intermediate and ventral grey matter (Fig. 3C). Rexed laminae I-III appeared normal as described previously in areas closer to the crush site, laminae IV-X showed patchy areas devoid of Nissl staining, and many neurons were observed in areas surrounding these patches. In the ventral horn at 1.5 mm from the crush, many motoneurons survived, however, the tissue surrounding these cells also contained patchy regions of necrosis. In parasagittal sections (not shown), neuronal loss extended an average of 700 μm (range; 630-750 μm) rostrally and 440 μm (range; 330-500 μm) caudally.

At 3 days survival time, the crush site in transverse sections appeared similar to 1 day in that no neurons were present within the crush site (not shown). In parasagittal sections, neuronal loss and tissue necrosis extended further distances bilaterally, dorsoventrally and rostrocaudally from the crush site compared to that seen at 1 day survival and averaged 830 μm (range; 750-880 μm) rostral and 500 μm caudal (range; 380-640 μm). Thus, areas closer to the crush showed some neuronal survival at 1 day survival appeared to be devoid of neurons at 3 days survival. Another distinguishing feature was the first appearance of small round, probably inflammatory cells at the crush. The number of these cells decreased with distance from the crush site. At further distances (1-1.5 mm), neuron loss was progressively less and occurred in small patches.

At 7 days survival, the most prominent feature in transverse and parasagittal sections was the invasion of large numbers of inflammatory cells, possibly microglia and macrophages, into the crush site and adjacent regions. The presence of these cells has been extensively demonstrated within and adjacent to an injury site after dorsal hemisection of the spinal cord (Dusart and Schwab, 1994). Infiltration of inflammatory cells made it difficult to

assess the degree of neuronal loss at the 7 days survival (Figs. 3D-F). Adjacent to the crush site (Fig. 3D), inflammatory cells were distributed throughout grey matter and extended into white matter. Further from the crush site, these cells were most numerous in laminae V-VII (Fig. 3E) and were fewer in the dorsal and ventral horn. In sections furthest away from the crush site (Fig. 3F), inflammatory infiltrate was less, but still persisted throughout grey and extending into white matter. In parasagittal sections, the extent of neuronal loss now encompassed larger areas reaching as far as 1280 μm rostral (range; 1250-1350 μm) and 920 μm caudal (range; 880-1000 μm).

V. 5. Connexin43 after compression injury

In sections through the lesion epicenter encompassing 1.5 mm on either side of the crush site, there were clear alterations in Cx43 immunostaining as seen in micrographs of parasagittal sections stained by the PAP method (Figs. 4A-D). At 1 day survival time, there was a total absence of Cx43 staining within the crush site (Fig. 4A). Adjacent to the crush site, Cx43 immunostaining was altered from generally evenly distributed puncta seen in normal tissue, to a more amorphous, reticular and intensified appearance. This intensified staining encompassed vast areas of grey matter extending from the superficial tip of the dorsal horn to the ventral tip of the ventral horn and extended an average of a 670 μm rostrally (range; 630-750 μm) from the crush site and 520 μm caudally (range; 380-630 μm). Beyond this intensified staining, there was a zone of Cx43 staining loss extending an average of 180-400 μm rostral and 80-330 μm caudal from the crush site. This zone of loss was adjacent to normal fine punctate staining furthest away from the crush site. Smaller areas of Cx43 loss were seen intermingled with normal staining furthest away from the lesion and increased closer towards the lesion resulting in a zone of Cx43 loss. These same

patterns of Cx43 immunostaining were observed in transverse sections (Figs. 4E-G), where compared to normal regions of staining (Fig. 4E), sections adjacent to the crush site showed intensified staining in large areas of grey matter (Fig. 4F). Patches of Cx43 immunostaining loss were interspersed in areas of intensified staining and less commonly near the center of the lesion, although small areas of Cx43-IR loss were seen immediately ventral to the substantia gelatinosa and dorsal to the ventral tip of the ventral horn. Patches of Cx43 immunostaining loss were more commonly distributed in areas of normal fine punctate staining further away from the lesion (Fig. 4G), and were of various sizes, being smaller further away from the crush and increasing in size progressively towards the crush site. Intensified staining did not extend as far away from the lesion as did the loss of immunostaining which occasionally extended all the way out to 1.5 mm. Thus, intensified and loss of staining appeared to be mutually exclusive and non-overlapping with the loss occurring adjacent to normal labelling and the intensified staining occurring adjacent to the crush site. In transverse sections furthest away from the crush site, the most dramatic change was an absence of staining for Cx43 in the most ventral portion of the dorsal column and the first appearance of intensified, amorphous staining around the central canal (not shown). Loss of staining also occurred in white matter and sometimes there was a continuity of loss extending from grey into white matter.

Qualitatively similar results were seen when the lesion encompassed a larger area such that Cx43 loss was proportionally larger and was seen further from the crush site, and intensified staining extended more rostral and caudal relative to the crush site.

At 3 days survival time, results derived from parasagittal and transverse sections paralleled the pattern of Cx43-IR observed at 1 day survival (not shown). Thus, progressively away from the crush site, loss of Cx43 staining was followed by intensified

staining, then a zone of Cx43 loss and then normal fine punctate staining beyond. The main difference from the 1 day survival time was that intensified staining was more sparse adjacent to the crush site and extended to further distances of 1060 μm (range;750-1380 μm) rostrally and 710 μm (range; 380-1000 μm) caudally from the crush site. The zone of Cx43 loss at 3 days extended an average of 120-300 μm rostrally (range; 100-350 μm) and 130-450 μm caudally (range; 80-450 μm).

At 7 days survival time, the most dramatic change was a total disappearance of Cx43-IR (Fig. 4C) in areas surrounding the lesion site and these areas were adjacent to normal staining at further distances. Regions devoid of Cx43 extended an average of 1100 μm rostrally (range; 880-1250 μm) and 690 μm caudally (range; 630-750 μm). Thus, in comparison to the earlier survival times where the injury site was characterized by zones of intensified staining as well as loss of Cx43 staining, by 7 days the latter zone had expanded into the area earlier occupied by the former. Under control conditions with omission of the primary antibody, no labelling was seen in sections processed with secondary and third antibodies (Fig. 4D) indicating the absence of background staining or endogenous peroxidase activity at the lesion site.

V.6. Connexin43 and neuron loss after compression injury

To compare areas of neuronal loss with Cx43 expression, adjacent sections were taken for Nissl staining and Cx43 immunofluorescence with antibody 18A-8 or sections were stained for Cx43 with antibody, followed by counterstaining with ethidium bromide. In comparisons of adjacent sections at 1 day survival, areas with loss of 18A-8 staining (Figs. 5A and B) corresponded to those with loss of neurons (Figs. 3B and C). Thus, the Cx43 staining at 750 μm from the crush site was evident where neurons were present and absent

in regions of neuron loss (compare Figs. 3B and 5A). In sections further away from the crush site (Figs. 3C and 5B), 18A-8 was lost in patches (Fig. 5B) corresponding to the patches devoid of neurons (Fig. 3C). Similar results were obtained in sections processed with 18A-8 and counterstained with ethidium bromide (Fig. 6). In control animals, Cx43 had a typical fine punctate appearance in regions of the dorsal horn (Fig. 6A) containing a normal distribution of neurons (Fig. 6B). At 1 day survival time, the persistence of normal Cx43 staining adjacent to the crush site in the dorsal and ventral tips of grey matter was accompanied by an abrupt absence of Cx43 in adjacent areas, and intensified staining was seen adjacent to the absence of Cx43 staining (Fig. 6C). Areas of normal staining in laminae I and II of the dorsal horn contained many neurons (Fig. 6D); however, in comparison to control sections neuronal numbers were somewhat reduced. The area of abrupt loss of Cx43 immunostaining immediately ventral to normal staining was devoid of neurons, as was the region of intensified staining ventral to the loss of Cx43-IR. Intensified staining was always associated with neuronal loss. Further from the crush site, in areas of normal Cx43 staining, neuronal staining had a relatively normal appearance in that smaller, more densely packed cells were seen in the substantia gelatinosa and Rexed lamina I, III and IV. Neurons surrounded by areas of neuron loss were seen in intermediate and ventral grey matter. Patches of Cx43 loss were more sparsely distributed further away from the crush site.

Similar relationships between Cx43 staining and neuron loss were seen at 3 days as described at 1 day survival (not shown). Thus, areas of intensified Cx43 or loss of Cx43 immunostaining adjacent to and some distance from the crush site were associated with massive neuronal loss.

At 7 days survival time, as also seen in Nissl stained sections, areas at and adjacent to the crush site were consistently filled with large numbers of round cells that appeared to be

macrophages or reactive microglia. Borders between areas exhibiting normal and loss of Cx43 labelling, such as the dorsal and ventral horn tips of grey matter (Fig. 6E), were clearly delineated by an accumulation of these round cells where Cx43 staining was absent (Fig. 6F).

V.7. Intensified staining with 18A-8 and 16A-8

Both the 18A-8 and 16A-8 antibodies showed immunostaining alterations from a normally fine, dense punctate appearance to a more intensely stained, amorphous and reticular pattern described at 1 and 3 days survival, and labelling with both was absent at 7 days survival. Higher magnifications revealed that individual immunostained elements were much larger and less punctate. Fig. 7A shows a normal area adjacent to intensified staining with 18A-8. Similarly, intensified immunostained elements with 16A-8 had irregular sizes and were often circular in nature with their centers unstained (Fig. 7B). Similar to the annular profiles seen in normal tissue, the diameter of these annular profiles ranged from 1-8 μm, and these profiles were only observed in grey matter at and near the lesion site. Detailed examination revealed no differences in the morphological appearance of intensified 18A-8 and 16A-8 staining.

V.8. Comparisons of antibodies 18A-8 and 16A-8 after compression injury

In unaffected areas of the cord, antibody 16A-8 produced similar staining patterns as 18A-8 except that the staining was somewhat weaker as occurs elsewhere in the CNS. Since lesions in brain generally give rise to the loss of 18A-8 staining, but are accompanied by an increase in 16A-8 staining, we tested whether areas of loss of 18A-8 staining in the spinal cord corresponded to those with elevated 16A-8 staining.

At 1 day survival time, adjacent sections were stained for 18A-8 and 16A-8 or simultaneously each with GFAP. It was found that areas showing loss of 18A-8 staining corresponded exactly to those with increased 16A-8 staining (Figs. 8A-D). This is consistent with the observation that no loss of staining was observed with 16A-8 as occurred with 18A-8. Thus, in the dorsal horn, areas of 18A-8 loss ventral to normal fine punctate staining (Fig. 8A) were filled by 16A-8 staining (Fig. 8B), the intensity of which was greatly increased. Intensified 16A-8 staining in the intermediate grey matter (Fig. 8D) had a very similar distribution as pockets of 18A-8 loss (Fig. 8C). Comparisons of adjacent sections also showed that areas of normal 18A-8 staining were associated with the presence of GFAP (compare Figs. 8A and E), whereas regions of 18A-8 absence and intensified 16A-8 staining were associated with GFAP loss (compare Figs. 8C, D and F).

Comparisons of staining with antibodies 18A-8 and 16A-8 at 3 days survival near as well as further away from the crush site indicated similar results (not shown) to those described at 1 day survival. Thus, staining with 16A-8 was evident in patches where 18A-8 staining was absent. This was also true in white matter. For example, in ventral aspects of the dorsal column where staining for 18A-8 was invariably lost in all sections at the crush site, immunostaining with 16A-8 was present, although sparse, and had a typical punctate appearance. Increased 16A-8 staining in peripheral regions of lateral and ventral white matter was also present where 18A-8 staining was largely absent or much less. The presence of intensified 16A-8 staining in white matter was also invariably associated with loss of staining for GFAP.

. Immunostaining for Cx43 with antibody 16A-8 at 7 days survival was similar to that observed at 3 days in that 16A-8 staining appeared to be present, but much more sparsely, in areas of 18A-8 absence (not shown).

V.9. Connexin43 and astrocytes after compression injury in grey matter

Detailed descriptions of astrocytes and their distribution in grey matter of normal cord have been previously reported (Bodega et al., 1986; Hajos et al., 1989; Liuzzi et al., 1987). Generally these are referred to as either protoplasmic (Bodega et al., 1986) or stellate (Hajos et al., 1989) based on morphological criteria. They are uniformly distributed in the dorsal and ventral horn with the exception of the periependymal condensation (Hajos et al., 1989) and the increasingly dense glial populations towards the substantia gelatinosa (Bodega et al., 1986).

An example of Cx43 and astrocytes in the intermediate laminae of the normal spinal cord grey matter is presented in Figs. 9A and B, respectively. In sections simultaneously stained for Cx43 and GFAP, fine Cx43-immunopositive puncta (Fig. 9A) were seen throughout areas of GFAP-positive astrocytes (Fig. 9B). Three days after compression injury, areas containing normal Cx43 staining (Fig. 9C) were fully occupied by reactive astrocytes as indicated by their intense staining for GFAP, swollen cell bodies and short processes (Fig. 9D).

At 1 day survival time, loss of Cx43 and GFAP staining in the grey matter at the crush site was already extensive and loss of Cx43 staining (Fig. 10A) corresponded with areas devoid of GFAP staining (Fig. 10B). GFAP staining was also absent in areas adjacent to the crush site where Cx43 staining was of the intensified annular profile type. Thus, regions characterized by annular profile staining could well predict the absence of GFAP. Moreover, since there was a transition between loss of 18A-8 staining to the appearance of annular profile staining and since loss of 18A-8 as well as the presence of annular profiles staining were both always accompanied by a loss in GFAP, it can be inferred that annular profile staining rarely bordered regions of GFAP staining. This in fact was the case, such

that annular profile and GFAP staining were always separated from each other by a region totally devoid of staining. For example in the ventral horn, normal staining (Fig. 10C) in areas of GFAP-positive astrocytes (Fig. 10D) was adjacent to a total absence of staining, which in turn was adjacent to annular profile/intensified staining devoid of GFAP closer to the crush site. In contrast, at borders between the presence and absence of GFAP, there was a good correlation between the presence and absence of Cx43. At these borders, GFAP-positive cells were considered to be reactive astrocytes. Their cell bodies were not as large as those of typical reactive astrocytes, but they tended to have more processes and were larger than normal astrocytes. Reactive astrocytes consistently bordered regions of GFAP loss in white or grey matter whether this occurred in vast areas of GFAP loss close to the lesion or at only small patches of GFAP loss further away from the lesion. Beyond these borders of reactive astrocytes, GFAP staining and astrocytes appeared normal.

At 3 days survival time, it was impossible to assess the state of the astrocytes within and near the crush site, since large regions were devoid of GFAP as well as Cx43 staining. Similar to the 1 day survival, areas immediately adjacent to the crush site containing annular profiles were also devoid of GFAP. Reactive astrocytes were clearly present at some distance from the crush site where both Cx43 and GFAP were evident around patches where both were absent. In these areas, Cx43 staining was reduced, but otherwise had a normal appearance. Thus, these regions further away from the lesion demonstrate that normal staining for Cx43 occurs in association with reactive astrocytes. Reactive astrocytes were also present even further away from the crush site where there did not appear to be a reduction of Cx43.

At 7 days survival time, all grey matter and central regions of the spinal cord were devoid of Cx43 and GFAP staining.

V.10. Connexin43 and astrocytes after compression injury in white matter.

Astrocytes are present throughout white matter regions of normal spinal cord. They extend endfeet to form the glial limitans in the dorsal column, lateral and ventral funiculi and radial glial cells surround the periphery of the cord. For more detailed descriptions of astrocytes in white matter see Bodega et al. (1986) and Liuzzi et al. (1987).

In control animals, fine Cx43-immunopositive puncta were distributed throughout the dorsal column (Fig. 11A) and were occasionally associated with GFAP-positive astrocytes (Fig. 11B). At 1 day survival time, Cx43-immunopositive puncta (Fig. 11C) in the dorsal part of the dorsal column were more strongly associated with reactive astrocytes (Fig. 11D) which were seen radiating towards the crush site and there appeared to be a good correspondence between the presence of Cx43 and reactive astrocytes. In the ventral aspect of the dorsal column, staining for both Cx43 and GFAP was largely absent. In contrast to observations at 1 day, at 3 days survival, reactive astrocytes (Fig. 11F) having plump cell bodies, short processes and intense GFAP staining were present in the dorsal aspect of the dorsal column where Cx43 staining persisted, but also extended ventrally where Cx43 was clearly absent (Fig. 11E).

In the ventral and lateral white matter, there was also a strong association between the presence of Cx43 and GFAP-positive astrocytes (Figs. 12A-F). In control animals, Cx43-immunopositive puncta (Fig. 12A) were seen along GFAP-labelled bundles of myelineated fibers emanating from the ventral horn grey matter (Fig. 12B). This correspondence was also seen in the lateral funiculi and to a lesser extent in the dorsal aspect of the dorsal column (refer to Figs. 11A and B). Similar areas after compression injury at 1 day survival time showed a close correspondence between Cx43 (Fig. 12C) and GFAP labelling (Fig. 12D) at the peripheral edge of the ventral white matter. In the same

section more dorsally, staining for both Cx43 and GFAP was absent. At 3 days survival time, although there was strong GFAP staining at the periphery of lateral white matter (Fig. 12F), Cx43 immunolabelling was sparse and peripheral regions of white matter were largely devoid of Cx43 (Fig. 12E), but some GFAP-positive cell bodies with centrally directed processes were associated with Cx43-immunopositive puncta.

At 7 days survival time, Cx43 (Fig. 13A) in many white matter regions further away from the crush site, was evenly distributed in areas where astrocytes were present (Fig. 13B). In areas closer to the crush site, Cx43 was associated with blood vessels (Fig. 13C) and with GFAP-positive fibers radiating centrally (Fig. 13D). These GFAP fibers were less dense and appeared to be less prolific than those observed at 3 days survival, and appeared to be absent in many regions close to the crush site. In fact, virtually the entire spinal cord including the peripheral rim was devoid of GFAP-positive fibers at and very near the crush site. It appeared that GFAP fibers seen radiating inward at 7 days had not progressed beyond a short distance, while most others had disappeared. However, in some white matter areas closer to the crush site, GFAP-positive processes were present, appearing to have penetrated inwards, but labelling was more sparsely distributed than seen in normal white matter. One exception to the correlation between the presence of Cx43 and GFAP was along blood vessels. At or very near the crush site blood vessels exhibited Cx43-immunoreactive puncta, but not GFAP staining (not shown). Blood vessels penetrating radially into the cord from peripheral regions were almost always immunoreactive for Cx43 (Fig.13C, E) and laden with GFAP-positive fibers (Fig. 13D). Cx43 was not distinctively associated with reactive astrocytes as at 3 days, or it was difficult to see this association despite the presence of reactive astrocytes. Punctate Cx43 labelling, particularly towards the periphery of white matter areas including dorsal column, lateral and ventral white matter,

had a honeycomb appearance, apparantly surrounding myelineated axons that remained intact. As at 3 days, but more so at 7 days, there was a stark demarcation between areas totally lacking Cx43 and GFAP and areas which remained intact and contained normal Cx43 and GFAP staining.

V.11. Connexin43 at further distances from the compression site

Since spinal cord sections at further distances from the crush site had a relatively normal appearance, only noteworthy features at the different survival times at the 1.5-7.5 mm distance are mentioned here. In sections immediately adjacent to the epicenter block (1.5-4.5 mm) at 3 and 7 days survival time, the most prominent changes were observed in the white matter. In dorsolateral, lateral and ventral white matter, Cx43-immunoreactive puncta along myelineated fibers leaving and entering the grey matter extended towards superficial regions about one-third the distance observed in normal cord sections (Figs. 14A and B). Processes of radial glial cells close to the glial limitans also appeared to be less intensely labelled. Overall, Cx43 staining in white matter was less intense and appeared disorganized. At further distances (4.5-7.5 mm), Cx43-immunostaining appeared normal in the dorsal, lateral and ventral funiculi. Radial glial cell processes were again associated with intense Cx43-immunoreactive puncta and myelineated fibers in white matter were heavily laden with Cx43-immunopositive puncta and extended the same distance peripherally as observed in normal cord.

As in grey matter of epicenter blocks of 1 and 3 days survival time, patches of Cx43 immunostaining loss were seen extending from lamina V to the ventral aspect of lamina VII closer to the epicenter block and became smaller and eventually disappeared at further distances (4.5 mm). Thus, it appeared that these patches of immunostaining loss are in

continuation with the patches observed in the epicenter block and can be used as an indication of the extent and severity of the lesion.

VI. DISCUSSION

An important long-term goal of our lab is to understand how intercellular gap junctional communication between various cell types in the CNS contributes to neural function in normal and pathological conditions. This task has been both facilitated by the discovery of connexins, the proteins that form gap junctions, and complicated by the identification of a family of approximately 12 different connexins. Thus, it has become necessary to identify the connexin proteins expressed in CNS and to determine their localization and expression at anatomical, cellular and subcellular levels. This has been achieved for the astrocytic gap junctional protein Cx43 and our work has provided novel insights into the organization of astrocytic gap junctions. In previous *in vivo* work we demonstrated dramatic alterations in astrocytic Cx43 after CNS injury and neuron loss. Our results have provided the basis for more focussed efforts on the following specific hypotheses: 1) The astrocytic gap junctional syncytial network is highly responsive to local environmental needs for K^+ spatial buffering as well as for intercellular movement of metabolites generated by neuronal activity such that Cx43 production, gap junction formation and patterns of intercellular communication within this network are under short and long-term regulation by factors eminating from neurons; 2) Following CNS injury, the syncytial network is reorganized in an attempt to promote recovery and in a manner reflecting both the underlying anatomical array of reactive astrocytes and the particular spatio-temporal demands for gap junctions determined by the nature of the injury; 3) Failure of gap junctional regulatory mechanisms in some conditions of pathology leads to excessive closure or elimination of gap junctions, compromises astrocytic spatial buffering and contributes secondarily to neuronal damage.

In support of the aforementioned hypotheses, the present study is the first to investigate astrocytic Cx43 in normal spinal cord and document its response after spinal cord trauma. We have shown that: 1) There was a heterogeneous distribution of Cx43 in normal spinal cord grey and white matter; 2) After sci, the density of immunolabelling for Cx43 was

intensified immediately adjacent to the crush site followed by a zone of Cx43 immunolabelling loss and normal staining; 3) Areas of loss with one sequence-specific antibody exhibited intensified staining with another antibody suggesting that some molecular change in Cx43 resulted in the masking of specific epitopes; 4) Areas of neuronal depletion corresponded with the loss of immunostaining with one of the Cx43 antibodies and 5) There was a total absence of labelling for Cx43 at 7 days post-sci extending up to 1 mm from the crush site.

VI.1. Connexin43 and spatial buffering after compression injury

Based on previous results in our lab and those of others (Naus et al., 1991; Rohlmann et al., 1993), we hypothesize that long-term regulation of astrocytic Cx43 production and requirements for gap junctions are determined by local environmental needs for K^+ spatial buffering as well as for intercellular movement of metabolites or regulatory signals. Since K^+ spatial buffering is thought to be critical for homeostatic control around neurons, it is likely that neuronal elements contribute to gap junctional regulation. Compression of the mammalian spinal cord results in an initial rise of extracellular K^+ followed by a substantial loss of K^+ from the site of the impact (Chesler et al., 1991). Thus, elevated levels of extracellular K^+ subsequent to neuronal damage could lead to an initial increase of Cx43 after spinal cord compression injury in an attempt to aid the cell-to-cell redistribution of this ion through "functional syncytia" of gap junctionally coupled astrocytes (Bennett and Goodenough, 1978; Dudek et al., 1983; Gardner-Medrin, 1986; Massa and Mugnaini, 1982). This process may limit neuronal injury and contribute to subsequent reparative events. Increased Cx43, as reflected by normal patterns but elevated staining density for the protein is to be distinguished from intensified Cx43 staining which refers to the reticular, amorphous and annular profile type staining observed adjacent to the spinal cord crush site. Increased expression of Cx43 has been demonstrated in ischemic striatal regions exhibiting limited neuronal damage (Hossain et al., 1994c) and 5 h after kainic acid (KA)

administration (Hossain et al., 1994a). In order to determine whether Cx43 is increased in the acute phases after compression injury, where it may play a role in the increased demands for K+ spatial buffering, earlier survival times will have to be examined. In the present study, Cx43-immunolabelling had a distinct pattern at and some distance from the crush site. Beyond areas of intensified annular profile type staining adjacent to the crush site, there was a zone of Cx43 immunostaining loss followed by normal staining furthest away from the crush site. Preliminary EM investigations show that the intensified staining observed at the crush site consisted of some gap junctional staining, but most was associated with other structures including internalized or partly internalized junctions, labelled non-junctional membranes and multivesicular clusters. Thus, the area of intensified staining characterized largely by non-junctional labelling and the zone of Cx43 immunostaining loss may represent reduced gap junctional coupling by astrocytes in an attempt to sever communication with their neighbours, thereby restricting the outward flow of potentially damaging metabolites. Similarly, the absence of Cx43 immunolabelling at 7 days post-sci may suggest a virtual absence of astrocytic junctional coupling resulting in segregation of the lesion site from normal tissue. This would be in agreement with our hypothesis that certain pathological conditions may lead to excessive closure or elimination of gap junctions which compromises spatial buffering and may secondarily contribute to neuronal damage.

VI.2. Connexin43 and neuron loss after compression injury

If Cx43 production, gap junction formation and patterns of intercellular communication are under short and long-term control by factors eminating from neurons, then damage to neurons should be reflected in the reorganization of gap junctional Cx43. In this study, areas of intensified Cx43 and immunostaining loss were characterized by neuron death, whereas areas of normal staining were associated with neuronal survival. Neuronal loss in areas of absence of Cx43-IR was observed in KA-injected thalamus (Hossain et al., 1994a) and severely affected ischemic regions (Hossain et al., 1994c), whereas neuronal survival was

evident in areas where Cx43 was normal or increased. By LM, areas of increased Cx43-IR exhibited a greater preponderance of astrocytic gap junctions around neuronal elements and increased intracellular immunostaining in astrocytes and their processes (Hossain et al 1994). Similarly, neuronal death in spinal cord was vast in areas of Cx43-IR loss, as well as in areas of intensified annular profile type staining immediately adjacent to the crush site. Since intensified staining under EM was found to be mostly of the non-junctional type and Cx43-IR loss may reflect a loss of gap junctional coupling, it is possible that the elimination of gap junctions and Cx43 immunolabelling may parallel neuronal loss and reflect dependence of Cx43 expression on astrocyte/neuron interactions. Several observations suggest that astrocytic Cx43 responses to spinal cord compression injury may represent neuron-dependent events: 1) Alterations of Cx43 were confined to regions of detectable neuronal damage; 2) Cx43 immunostaining profiles were correlated with degrees of neuronal loss; and 3) Astrocytic Cx43 immunostaining was virtually abolished in areas depleted of neurons. We suggest that these different Cx43 immunostaining patterns may reflect responses of astrocytes to various degrees of neuronal damage.

VI.3. Masking of 18A-8 epitope and intensified staining with 16A-8

The molecular basis for the loss of immunohistochemically detectable Cx43 with antibody 18A-8 after sci is at present uncertain. It has previously been suggested that altered 18A-8 antibody recognition could be due to altered cellular localization of Cx43, internalization or partial degradation resulting in altered sensitivity of epitopes to tissue fixatives (Hossain et al., 1994). This seems unlikely since Cx43 protein remains intact at lesion sites as demonstrated by Western blot (Hossain et al., 1994a), and epitope masking occurs at intact astrocytic gap junctions as well as internalized junctions (Ochalski et al, 1995) as seen by EM. Moreover, it was found by in situ transblotting that altered epitope recognition occurs in fresh, unfixed tissue (Sawchuk et al., 1995). Masking of the 18A-8 epitope and increased exposure of the 16A-8 epitope has previously been demonstrated in

KA-lesioned tissue (Hossain et al., 1994). It appears that depending on the cellular functional state, Cx43 can undergo a molecular transformation such that epitopes readily recognized by antibody at one state are hidden in another and those ordinarily hidden become exposed. Hence, weaker immunolabelling of 16A-8 in normal spinal cord tissue is characterized by stronger 18A-8 labelling and areas of 18A-8 immunolabelling loss after sci exhibit intense 16A-8 staining. Masking of the 18A-8 and increased exposure of the 16A-8 epitope may be due to conformational or covalent modifications of Cx43 at or near these epitopes. The former is unlikely given the persistence of Cx43 epitope masking in in situ transblots treated with denaturing conditions (Sawchuk et al., 1995). The latter cannot be excluded given multiple Cx43 phosphorylation sites; subtle changes in these may go undetected by Western blots. Alternatively, altered epitope recognition may be due to the non-covalent association of a protein with the cytoplasmically localized Cx43 carboxyl-terminal tail bearing the site-specific 18A-8 and 16A-8 antibody epitopes. Future endeavours regarding these questions will aim to establish the existence of such an association and to determine whether it is related to biochemical mechanisms underlying regulation of junctional coupling and Cx43 disposition. Based on the extremely rapid Cx43 dephosphorylation we observed in brain (Hossain et al., 1994b), one outcome may be the association of a phosphatase with Cx43, which might be relevant to epitope masking.

VI.4. Connexin43 and the presence and absence of astrocytes

After spinal cord compression and other CNS injuries, astrocytes transform into reactive cells, the function of which is not entirely understood. Typically reactive astrocytes are characterized by a high expression of GFAP and vimentin (Eddelston and Mucke, 1993). Reactive astrocytes in this study were observed as early as 1 day post-sci, largely paralleling the temporal and spatial immunostaining profile of Cx43. If differences in Cx43 immunostaining reflect the molecular regulation of Cx43, it is possible that several different

masked and exposed states of Cx43 exist and that these are determined in part by the physiological states of astrocytes. In normal spinal cord, uniform dense labelling is seen throughout areas containing GFAP-positive astrocytes. Similarly, Cx43 staining with a normal appearance, but reduced density, is seen in areas of GFAP-positive reactive astrocytes at some distance from the crush site. Interestingly, in areas close to the crush site associated with intensified annular profile type staining, 18A-8 loss and intensified 16A-8 staining corresponded with a loss of GFAP-immunoreactivity. In KA-induced injury, GFAP-positive reactive astrocytes accumulated around the lesion site, but as determined by EM, astrocytes within the lesion site remained devoid of GFAP-immunostaining until 14 days when GFAP-positive astrocytes began to reappear (Dusart et al., 1991). Immunohistochemical work (Li and Nagy, unpublished observations) with vimentin in focal ischemic tissue revealed the presence of GFAP-negative reactive astrocytes in damaged tissue. These observations suggest that loss of GFAP-immunostaining does not necessarily reflect the absence of astrocytes within a lesion site, but similar to 18A-8, may present a case of epitope masking. In spinal cord, preliminary EM investigations of intensified annular profile staining close to the crush site revealed the presence of reactive astrocytes. At 1 day post-sci, grey and white matter areas bordering absence of both Cx43 and GFAP staining, contained reactive astrocytes immunopositive for Cx43. It is thus reasonable to assume that reactive astrocytes in regions close to the lesion site were gap junctionally coupled. An example of increased Cx43 associated with reactive astrocytes was seen in the dorsal column at 1 day post-sci, whereas at 3 days, reactive astrocytes extended closer towards the lesion epicenter, where Cx43 was absent. Increased Cx43 at 1 day post-sci may represent astrocytic increases in gap junctional coupling in an attempt to deal with spatial buffering demands, metabolic changes and excitotoxin release due to spinal cord trauma, whereas

absence of Cx43 at 3 days post-sci could reflect downregulation or elimination of gap junctional communication in areas close to the lesion due to severe trauma. At 7 days post-sci there was again a good correlation between Cx43 and GFAP staining in peripheral white matter at the crush site, whereas grey matter regions were largely devoid of Cx43 and GFAP labelling. Thus, if Cx43 expression depends on the physiological state of astrocytes, then the different immunohistochemical staining patterns observed at different survival times post-sci may reflect these states, such that normal, absent, increased and intensified Cx43 immunolabelling may represent differences in astrocytic gap junctional coupling in response to specific environmental demands.

VI.5. General conclusion

In the present immunohistochemical study we investigated the distribution patterns of the astrocytic gap junctional protein Cx43 after spinal cord compression injury. Although the literature on gap junctional communication between astrocytes *in vitro* and *in vivo* is vast, this is the first *in vivo* report to use Cx43 immunohistochemical staining to document gap junctional coupling between astrocytes after sci. We have shown that Cx43 distribution is heterogeneous in normal cord, has a distinct immunostaining pattern after sci, and further suggested that these staining patterns may reflect different gap junctional states of normal and reactive astrocytes. The descriptive nature of this study is necessary to provide *in vivo* support for later functional studies on astrocytic junctional communication and Cx43 expression after trauma to the spinal cord. Ultimately, we want to establish that antibody recognition patterns of Cx43 reflect gap junctional communicative capacity, and to identify the factors that regulate junctional coupling. Research ongoing in our laboratory involves the use of cortical and hippocampal slices to examine Cx43-immunostaining patterns. In

slices perfused in standard CSF medium, Cx43 distribution patterns remained similar to those observed in brain (Yamamoto et al., 1991), and in "unhealthy" slices, subjected to reduced or inadequate perfusion, Cx43-immunostaining was lost in patches with 18A-8 and increased with 16A-8. These results are similar to observations made after KA-lesions (Hossain et al., 1994a) and spinal cord trauma. Thus, methods of dye- or tracer-transfer between astrocytes in slices subsequently taken for Cx43 immunolocalization with 18A-8 and 16A-8 may provide evidence that tissue areas devoid of immunostaining with 18A-8 also lack gap junctional coupling. Such results would prove that: 1) antibody 18A-8 is a powerful immunohistochemical indicator of astrocytic gap junctional uncoupling relevant to our *in vivo* studies; 2) point to the significance of 18A-8 epitope as a potential regulatory site within Cx43; and 3) allow loss of Cx43 staining with 18A-8 to be used as an initial assay for physiological conditions or substances that regulate gap junctional coupling within the astrocytic syncytium.

VII. FIGURES

VII. Figure 1

Fig. 1. Photomicrographs of Cx43 immunolocalization in cervical spinal cord of normal rat. **A:** Low magnification view of Cx43 distribution in white and grey matter. **B-D:** Magnifications showing a greater density of staining in the substantia gelatinosa (B, large arrows), than deeper layers (B, small arrow), linear arranged punctate labelling in Lissauer's tract (Lt) (C, arrows), and uniform labelling in the intermediate laminae (D). Note punctate and annular profile (B, small arrowheads) appearance of labelling in deep laminae and the preponderance of the latter in the substantia gelatinosa. **E:** Ventral horn showing a concentration of labelling in motor nuclei and around motoneurons (arrows). **F,G:** Localization of Cx43 among ependymal cells around the central canal (F, arrows) and along blood vessels in white matter (G, arrows). Magnifications: A, x40; B, x350; C, x200; D, x490; E,x80; F,x330; G,x200

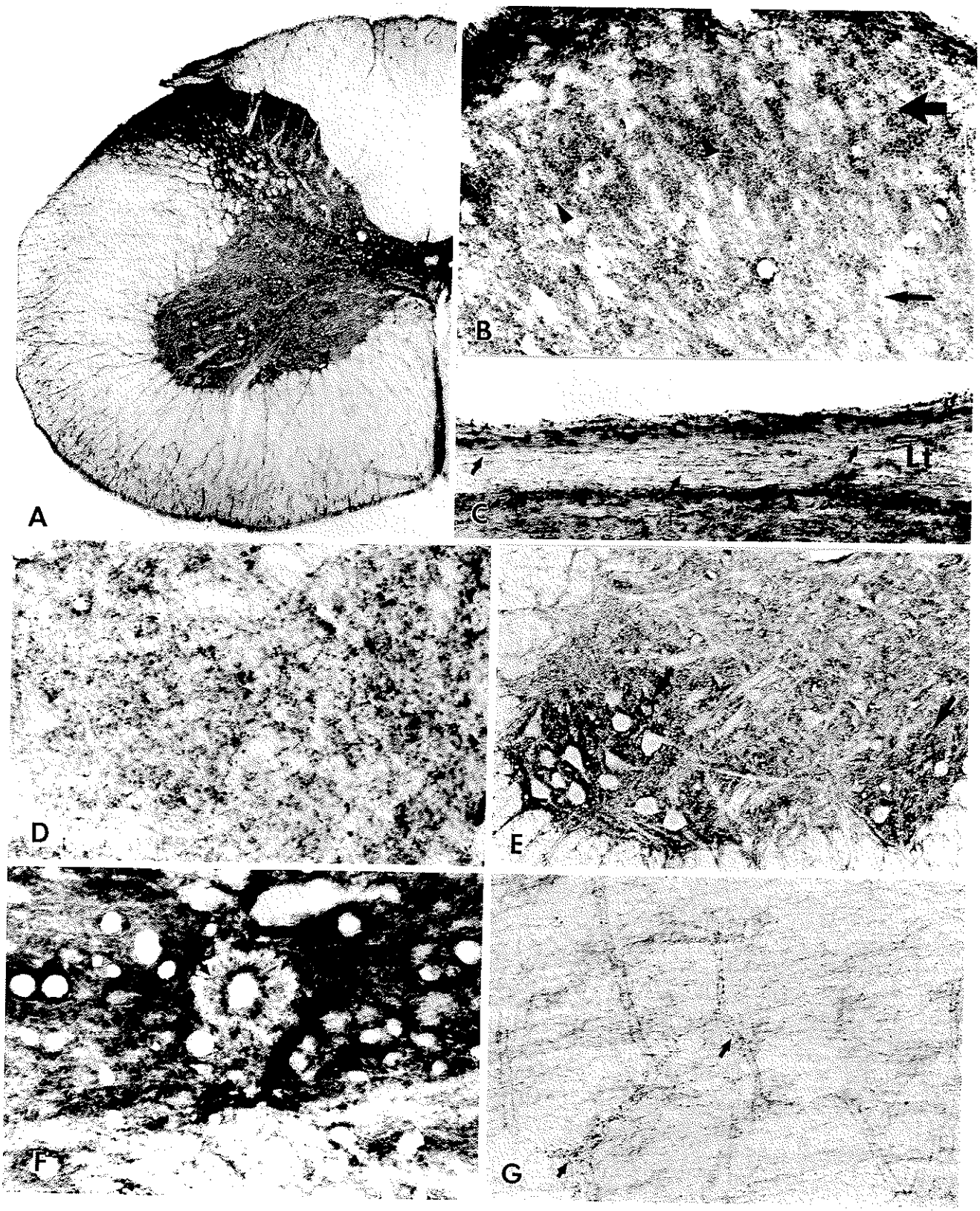

Fig.1

VII. Figure 2

Fig. 2. Photomicrographs of Cx43 distribution in white matter of cervical spinal cord in normal rat. **A-C:** In transverse sections, labelling is seen concentrated in fiber bundles (A, arrows) extending from the grey matter and, more superficially, is seen dispersed within (B, large arrows) or as puncta along (B, arrowheads) radial glial cells including their endfeet (B, small arrow) at the glial limitans where labelling (C, arrows) also appears to be associated with pial cells. **D,E:** In sagittal sections, Cx43 is seen along intermittantly labelled processes (arrows) travelling in the direction of myelinated fibers emerging from the dorsal column (D) or running rostro-caudally in the latter white matter (E). Magnifications: A, x170; B,C x360; D,E x300.

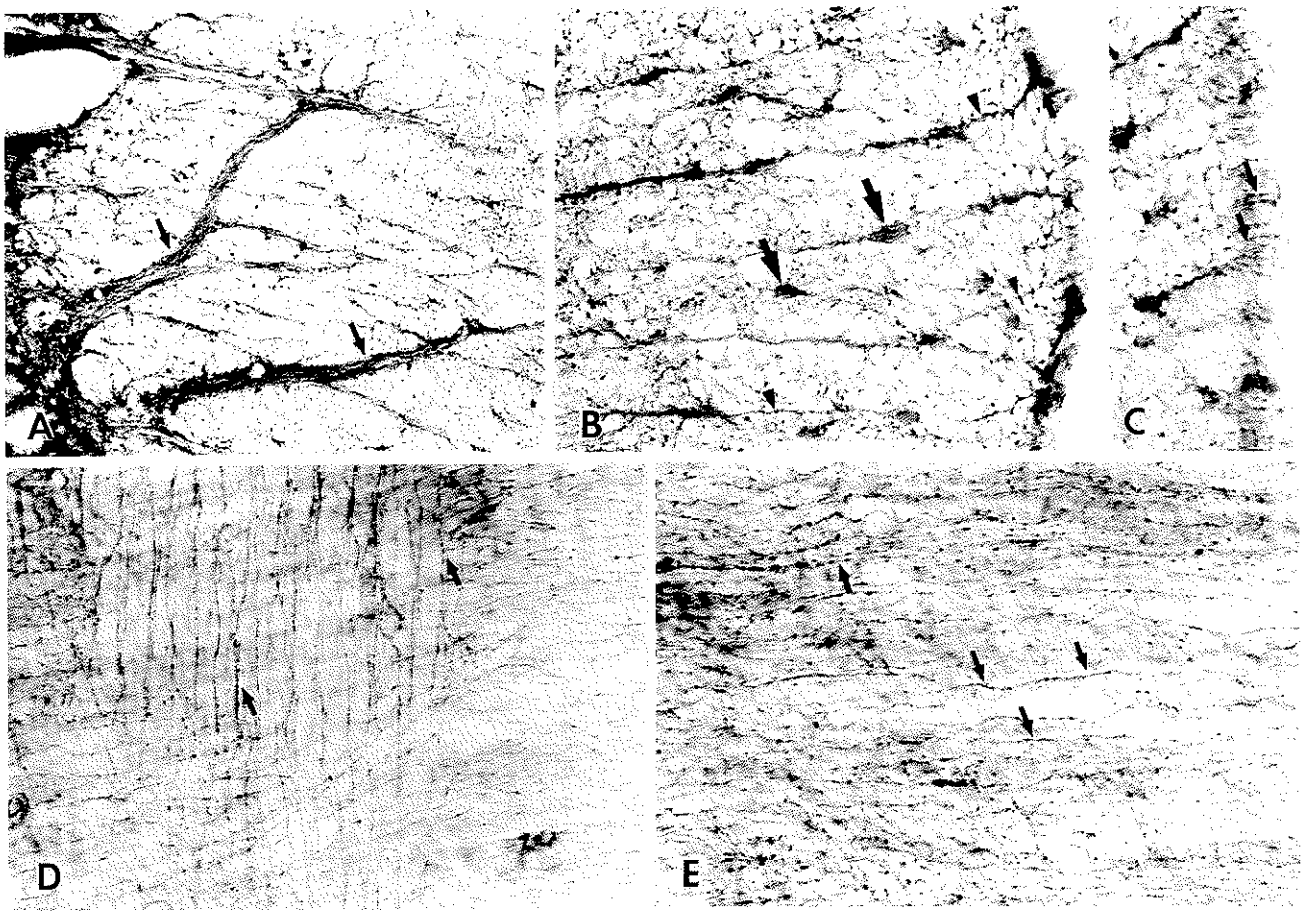

Fig.2

VII. Figure 3

Fig. 3. Nissl stained transverse sections of spinal cord showing extent of injury at various distances from the crush site. **A-C:** At 1 day post-injury, neuron loss (asterisks) occurs in nearly all grey matter areas adjacent to the crush (A), is most prominent in intermediate laminae at distances of 0.5 mm to 1 mm from the crush (B) and is limited to patches at further distances of 1 to 1.5 mm (C). **D-F:** At 7 days post-injury, areas of neuron loss at levels corresponding to those shown in A and B, respectively, are occupied by inflammatory cells (arrows in D,E). At further distances, these cells also invade the ventral aspect of the dorsal column (arrows in F). Magnifications: A-F, x40.

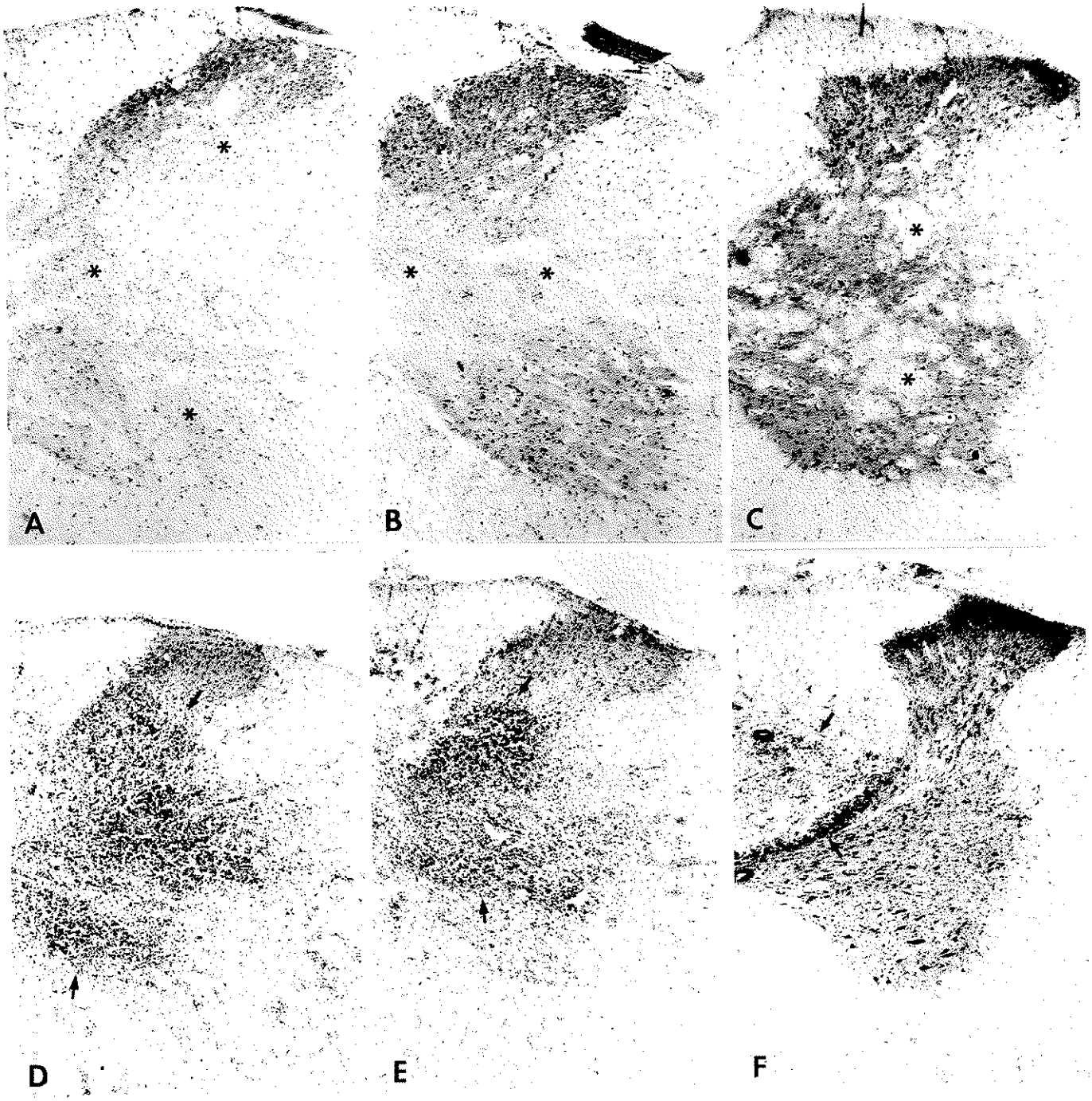

Fig.3

VII. Figure 4

Fig. 4. Saggital (A-D) and transverse (E-G) sections of spinal cord showing the distribution of Cx43-IR around the crush site. **A,B:** Low and higher magnification at 1 day post-injury. Labelling for Cx43 in grey matter is more sparse, but increased in intensity in areas adjacent to the lesion (arrowheads). In rostral and caudal zones flanking these areas, labelling is substantially reduced along a dorsovental strip (asterisks) beyond which it appears normal (star). **C:** At 7 days post-injury, labelling is absent in a wide zone (asterisks) extending from the crush. **E-G:** Transverse sections through a region of normal staining (E, corresponds to areas indicated by stars in A), a region of increased intensity of labelling (F, arrowheads, corresponds to areas indicated by arrowheads in A) and a level at the transition between reduced (asterisks) and normal staining (G). **D:** No labelling is seen in sections processed with omission of primary antibody. Magnifications: A-G, x30.

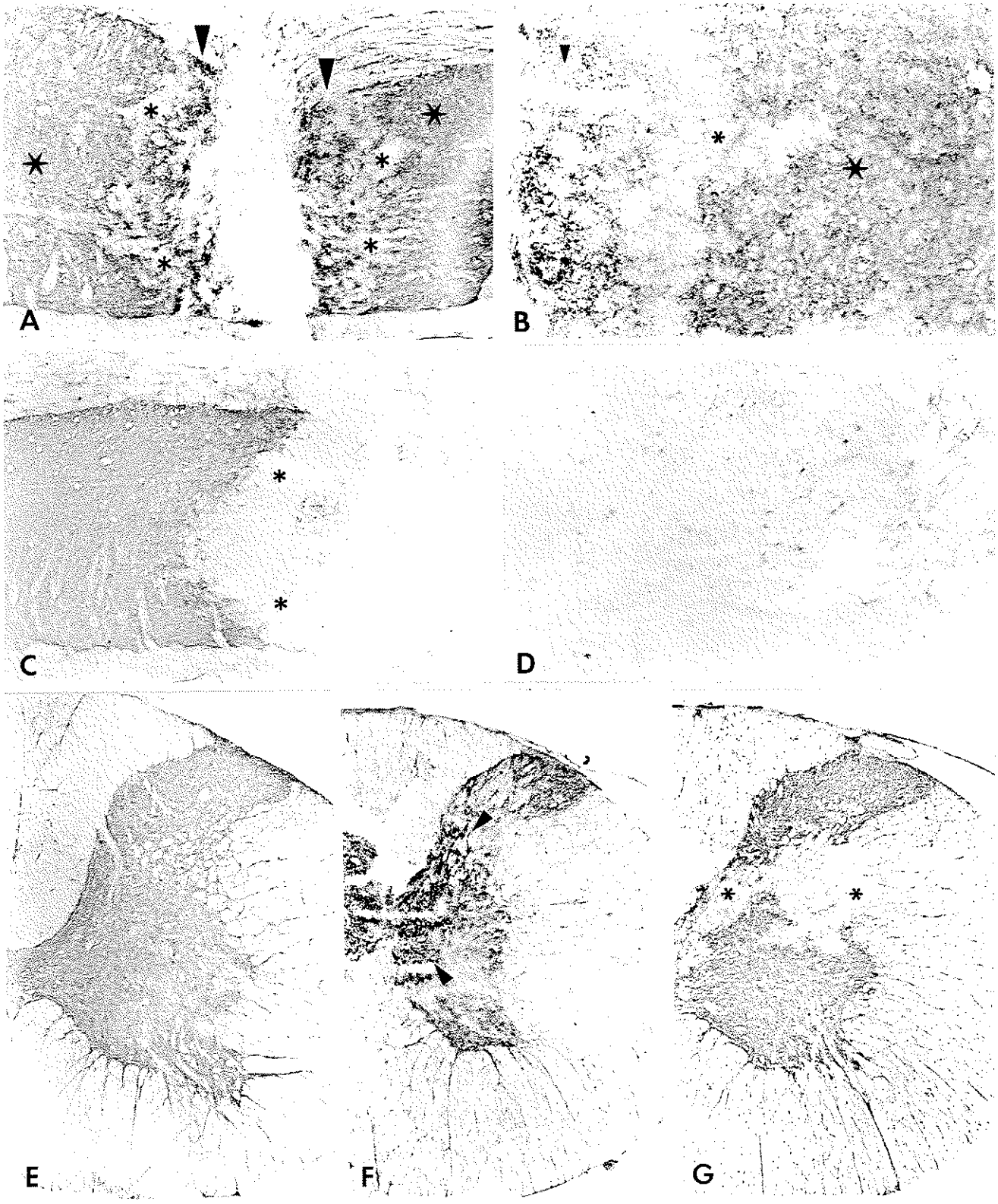

Fig.4

VII. Figure 5

Fig. 5. Distribution of Cx43-IR as related to extent of neuron loss at 1 day post-injury. **A,B:** Photomicrographs in A and B show Cx43 immunofluorescence in magnified areas of sections adjacent to, and at distances from the crush site, in the Nissl stained sections illustrated in Fig. 3B and C, respectively. Areas of reduced or an absence of labelling for Cx43 (asterisks) in these sections correspond to those exhibiting neuron loss (asterisks in Fig. 3B and C). Magnifications: A,B x60.

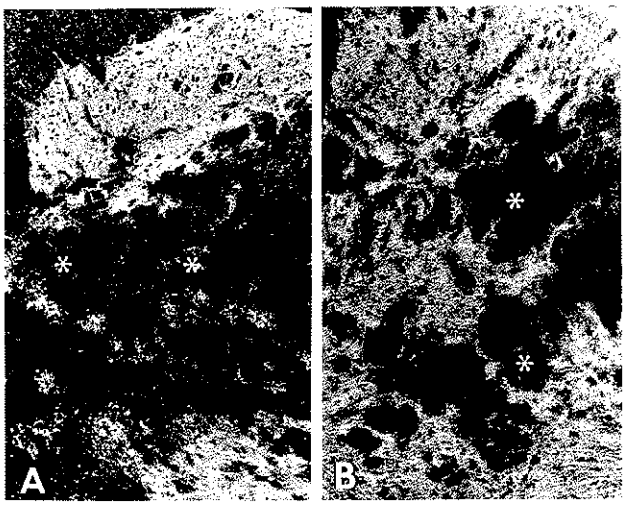

Fig.5

VII. Figure 6

Fig. 6. Cx43-IR and ethidium bromide staining in sections of normal dorsal horn with similar fields near a crush site. **A-D:** Unlike the relatively uniform labelling for Cx43 (A) and neurons (B) in normal tissue, a level slightly removed from the crush at 1 day post-injury (C) shows a transition from normal staining in superficial dorsal horn laminae (arrowheads), to a loss of labelling in immediately adjacent deeper layers (asterisks), to more intense, but less dense labelling in subjacent layers (arrows). Areas of Cx43 loss or intensified staining corresponded to areas of neuron loss (D). **E,F:** At 7 days post-injury, areas devoid of Cx43 (E, asterisks) contain ethidium bromide stained inflammatory cells (F, arrows). Magnifications: A,B x100; C-F x80.

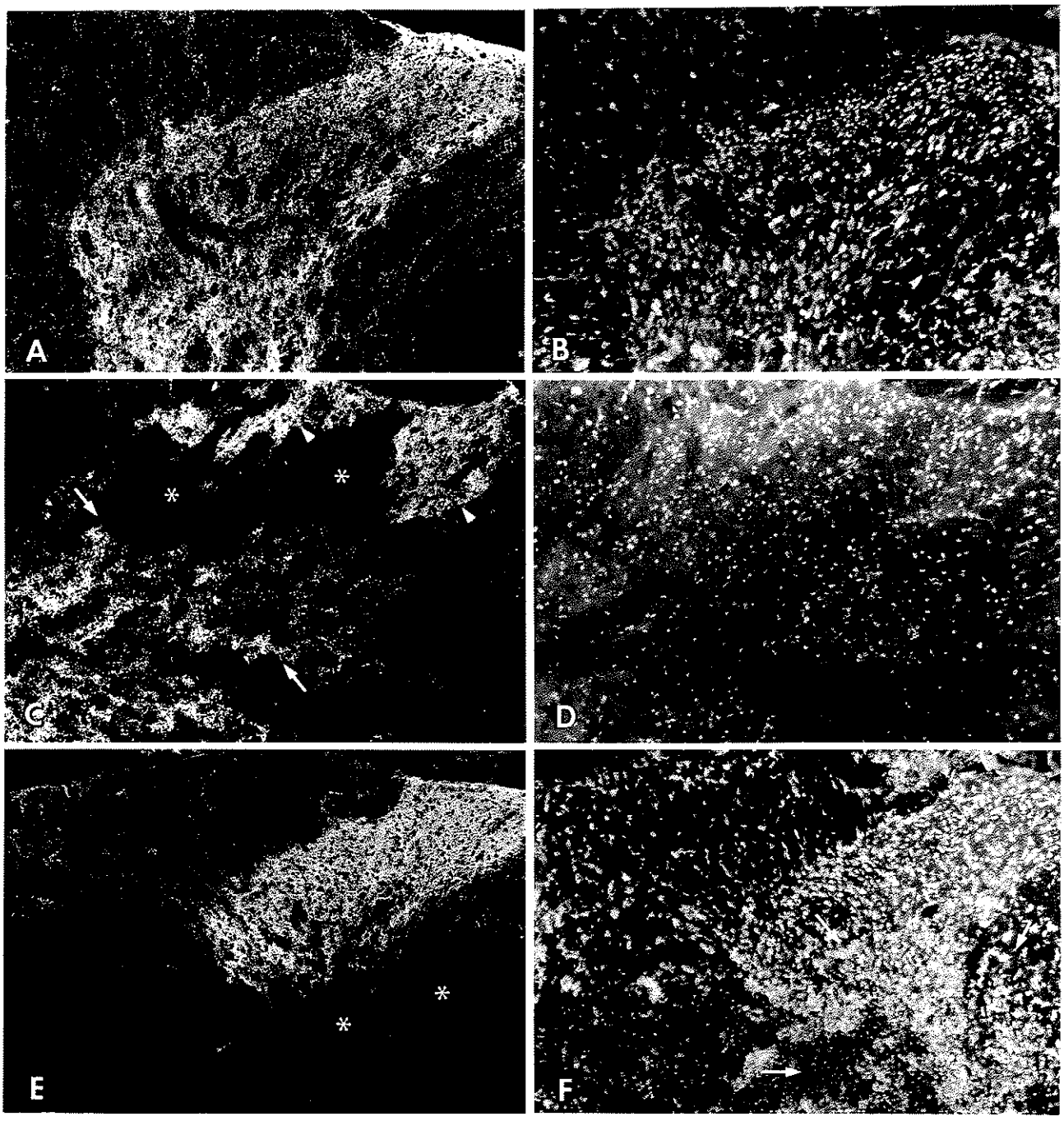

Fig.6

VII. Figure 7

Fig. 7. Higher magnification views of immunoperoxidase labelling for Cx43 in regions of normal (star) and more intense staining (arrows). **A,B:** As seen with both anti-Cx43 antibodies 18A-8 (A) and 16A-8 (B), labelling consists of some fine puncta and structures having the appearence of annular profiles (arrowheads). Magnifications: A, x180; B, x360.

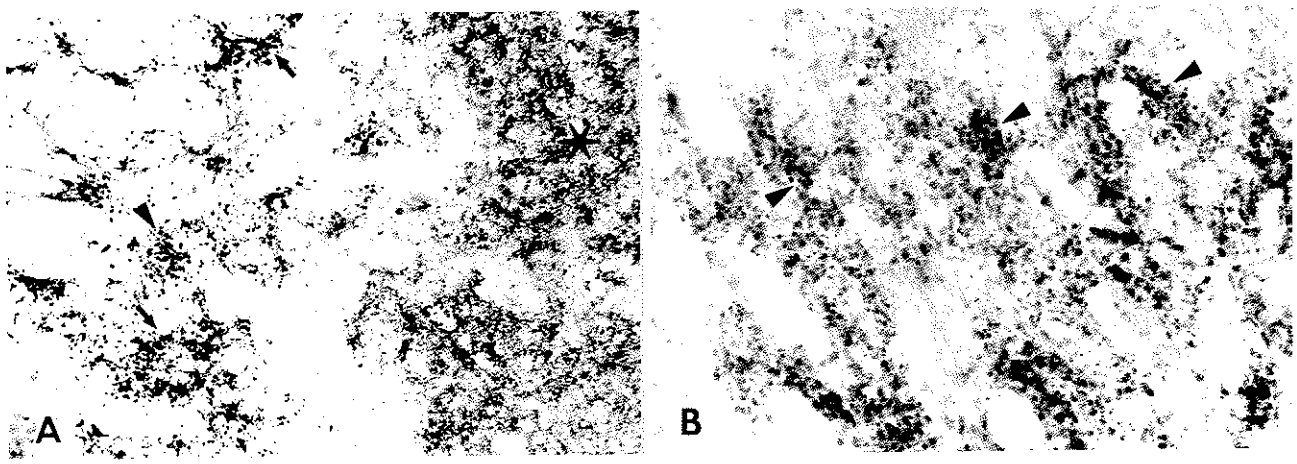

Fig.7

VII. Figure 8

Fig. 8. Immunofluorescence labelling with two different anti-Cx43 antibodies and with anti-GFAP near a crush site 1 day post-injury. **A-D**: Adjacent sections of the same field in dorsal horn (A,B) and adjacent sections of the same field in the ventral horn (C,D) immunostained for Cx43 with antibody 18A-8 (A,C) and 16A-8 (B,D). In both pairs of sections, areas with normal labelling with both Cx43 antibodies (stars) surround areas that are devoid of Cx43 labelling with 18A-8 (asterisks), but exhibit intensified staining with 16A-8 (arrows). **E,F:** Immunolabelling for GFAP in the same field of a section (E) adjacent to A and in the same field of a section (F) adjacent to C. Areas exhibiting loss of GFAP immunoreactivity in grey (asterisks) and white matter (double asterisks) correspond to those with altered Cx43 labelling. Magnifications: A, B x250; C,D x100; E,F x250.

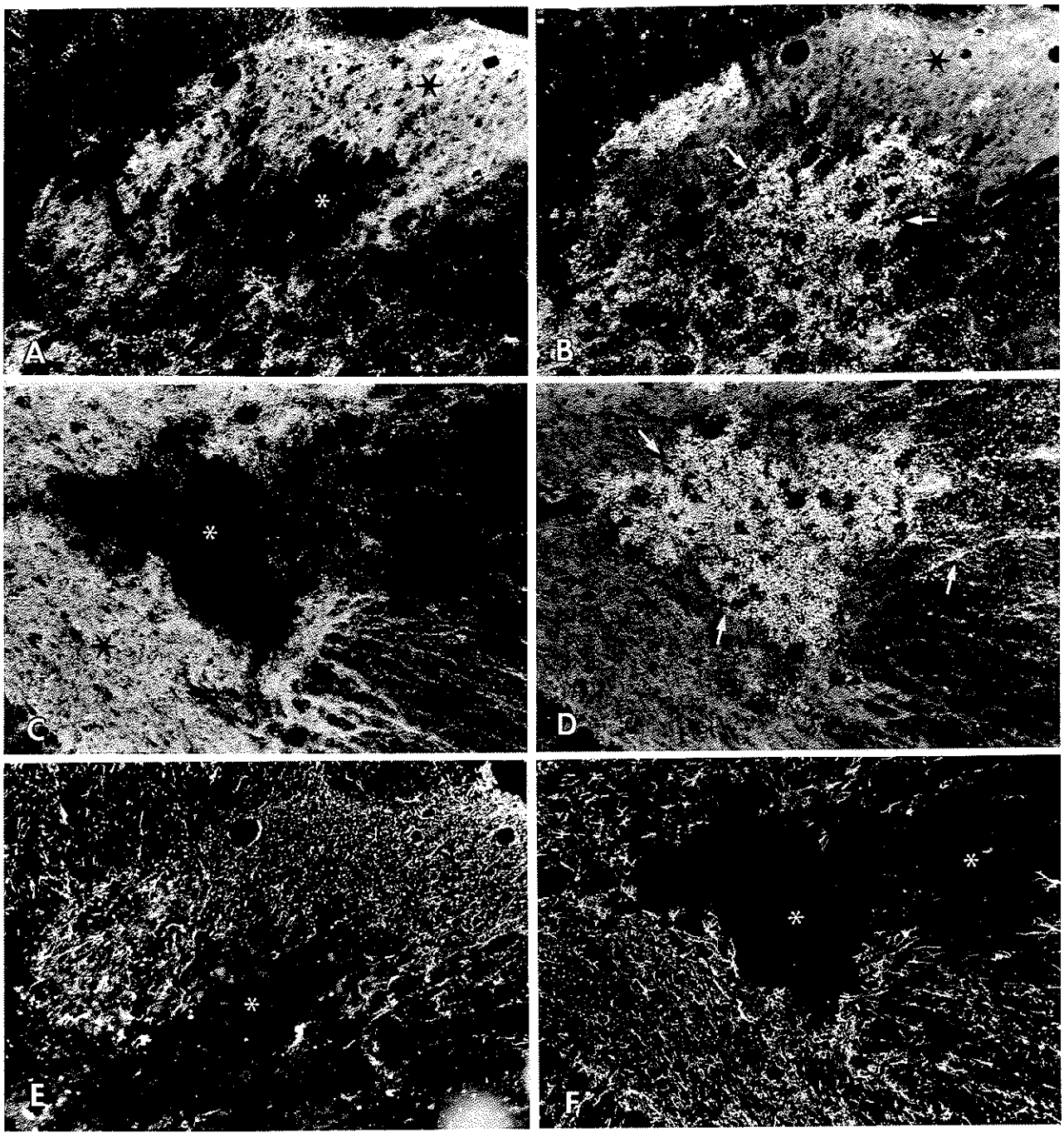

Fig.8

VII. Figure 9

Fig. 9. Comparison of labelling for Cx43 and GFAP in intermediate laminae of normal spinal cord grey matter with that in injured cord corresponding to a similar distance from a crush site shown in Fig. 1C. **A,B:** In normal tissue, uniformly dense labelling for Cx43 (A) is seen throughout areas containing GFAP-positive astrocytes (B). **C,D:** At this level removed from the crush site at 3 days post-injury, Cx43 labelling density is reduced (C), but otherwise has a normal appearence in areas occupied by reactive astrocytes exhibiting hypertrophy and intense labelling for GFAP (D). Magnifications: A, x250; B, x210; C,D x190.

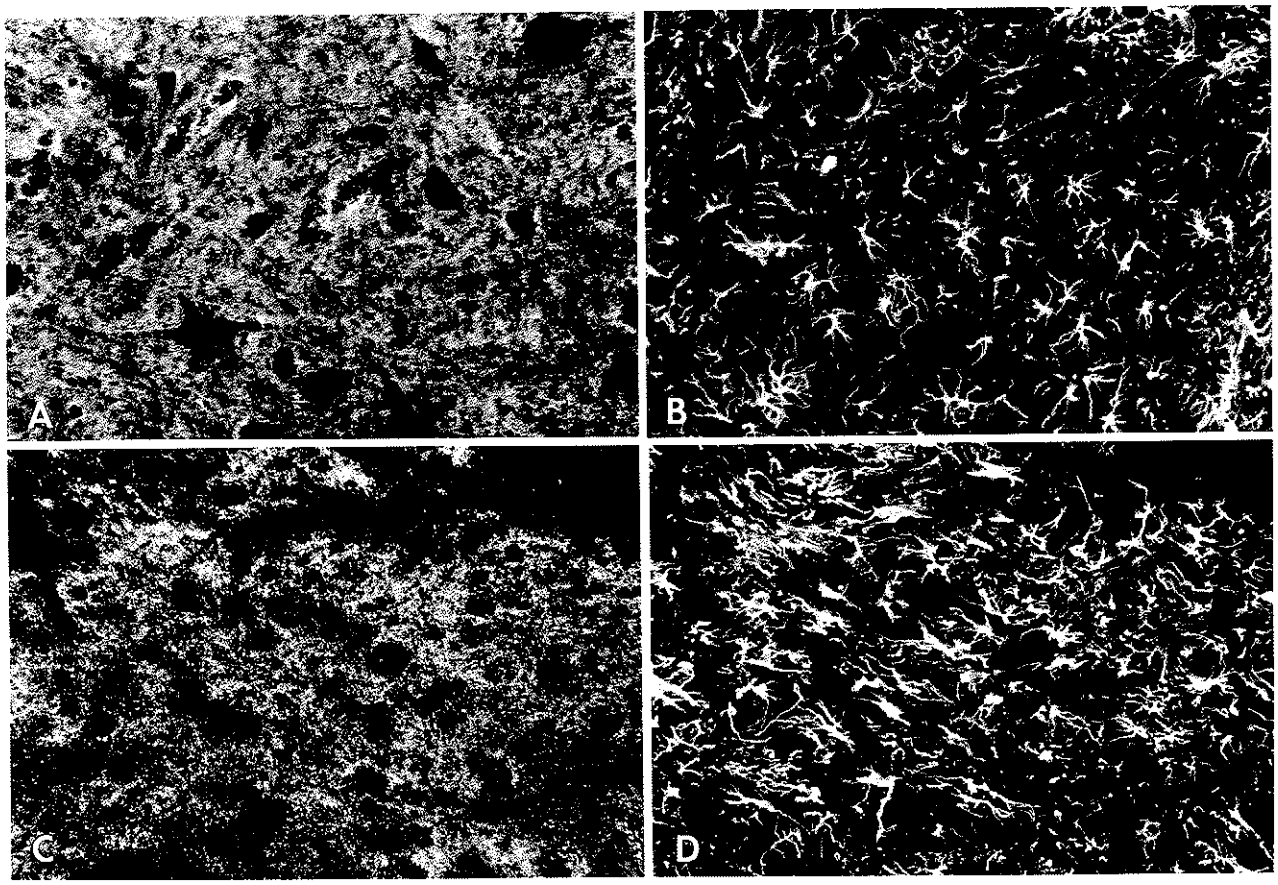

Fig.9

VII. Figure 10

Fig. 10. Pairs of immunofluorescence micrographs (A,B; C,D) showing labelling for Cx43 and GFAP in the same fields of dorsal and ventral grey matter adjacent to the crush site at 1 day post-injury. **A,B:** Areas of normal Cx43 labelling in the tip of the dorsal horn (stars) and an absence of staining more ventrally (A, asterisks) correspond with the presence (arrows) and absence (asterisks), respectively, of GFAP labelled astrocytes (B). **C,D:** In the ventral horn normal Cx43 labelling (star) is seen adjacent to areas of absence of staining (asterisks) and intensified staining (arrowheads) near the crush site (C). Areas of normal Cx43 labelling correspond to those immunopositive for GFAP (D, arrows) while those more medial with loss or intensified Cx43 lack GFAP (D, asterisks). Magnifications: A,B x110; C,D x100.

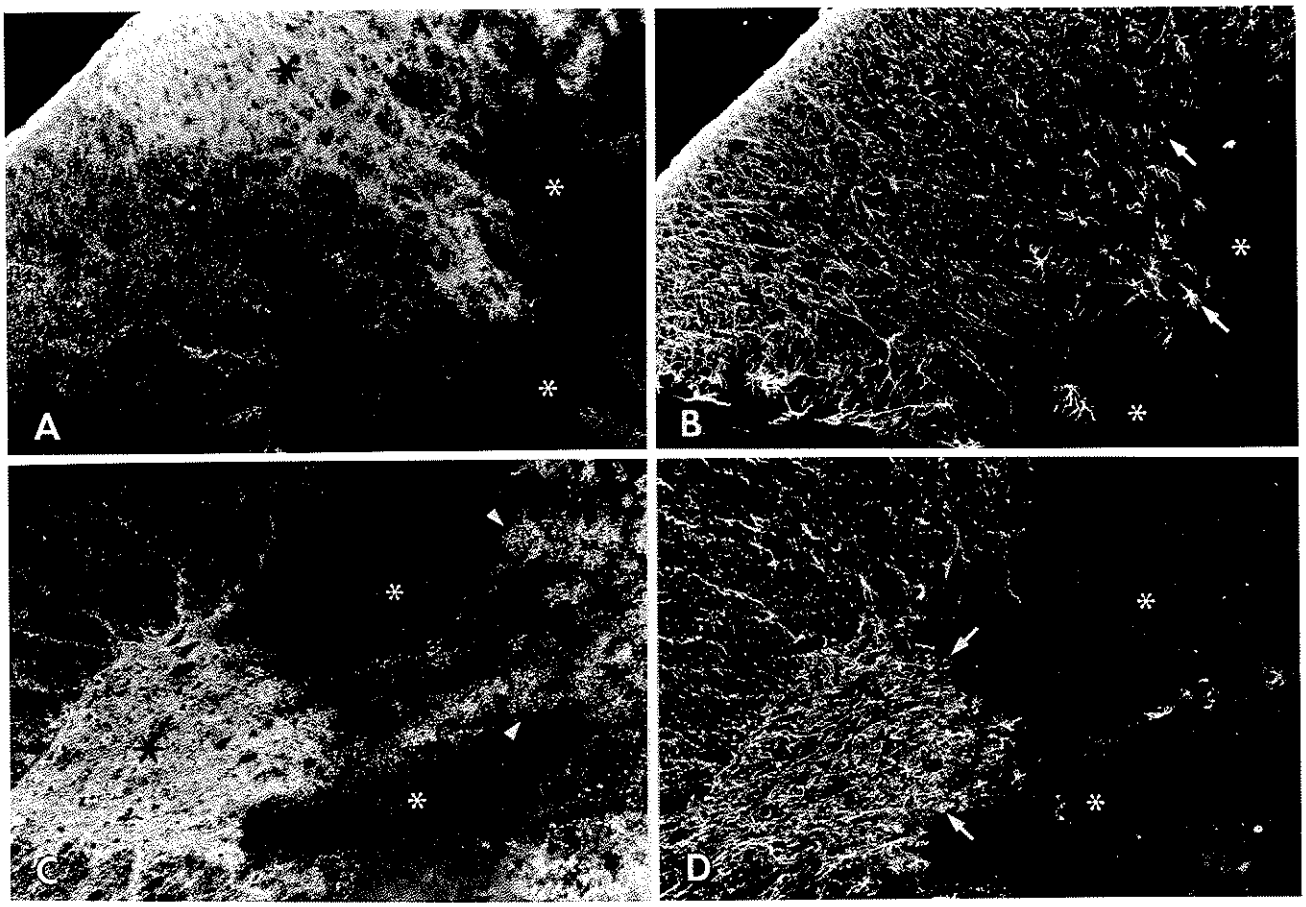

Fig.10

VII. Figure 11

Fig. 11. Labelling for Cx43 and GFAP in the dorsal column. Pairs of immunofluorescence micrographs (A,B; C,D; E,F) show the same fields immunolabelled for Cx43 (A,C,E) and GFAP (B,D,F) in normal tissue (A,B) and in a similar area of injured cord. **A,B:** In normal dorsal column, punctate Cx43 labelling is uniformly distributed (A) with occasional association (arrows) of puncta with GFAP-positive astrocytes (B). **C,D:** At 1 day post-injury, Cx43 (C, asterisks) and GFAP (D, asterisks) labelling in the ventral part of the dorsal column is largely absent, and Cx43 labelling in dorsal regions corresponds to the distribution of GFAP-positive astrocytes (arrows). **E,F:** At 3 days survival, Cx43 staining in ventral regions remains absent (E, asterisks) in areas containing reactive astrocytes (F, arrows). Magnifications: A, B x170; C, D x110; E,F x170.

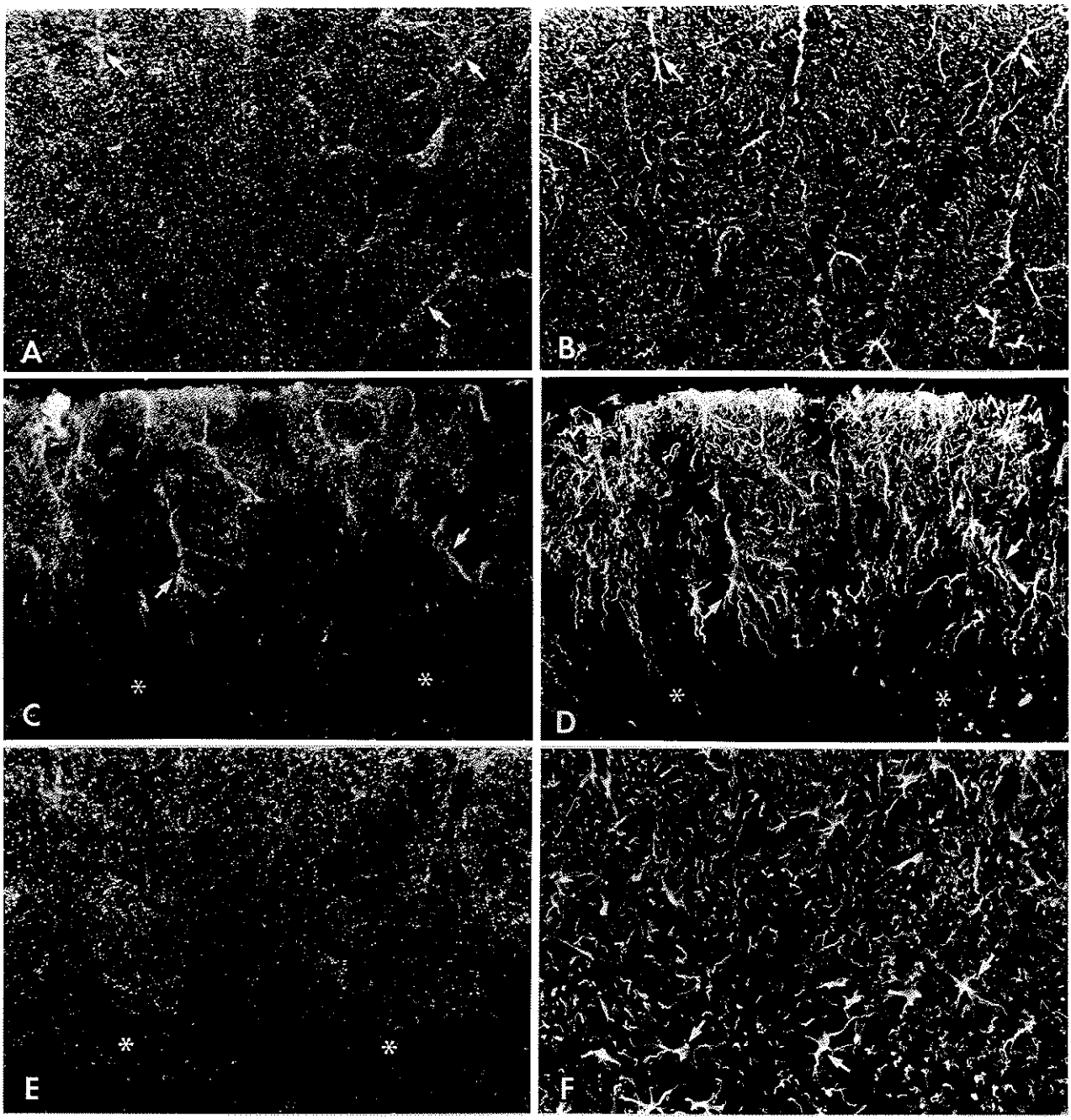

Fig.11

VII Figure 12

Fig. 12. Labelling for Cx43 and GFAP in ventral and lateral white matter. Pairs of immunofluorescence micrographs (A,B; C,D; E,F) show the same fields stained for Cx43 (A,C,E) and GFAP (B,D,F). **A,B:** Normal ventral white matter showing association of Cx43 (A, arrows) with GFAP-labelled (B, arrows) bundles of fibers eminating from the ventral horn (vh). **C,D:** Similar area as A,B at 1 day post-injury. Labelling for Cx43 (C, asterisks) and GFAP (D, asterisks) is absent in the central half of white matter, but exhibits a close correspondence in the peripheral half (arrows). **E,F:** Lateral white matter at 3 days post-injury showing a large reduction of Cx43 staining (E, asterisks) in a field of intensely stained GFAP-positive astrocytes (F) and the association of some Cx43 labelling (E, arrows) with some of these astrocytes (F, arrows). Magnifications: A,B x90; C,D x100; E,F x190.

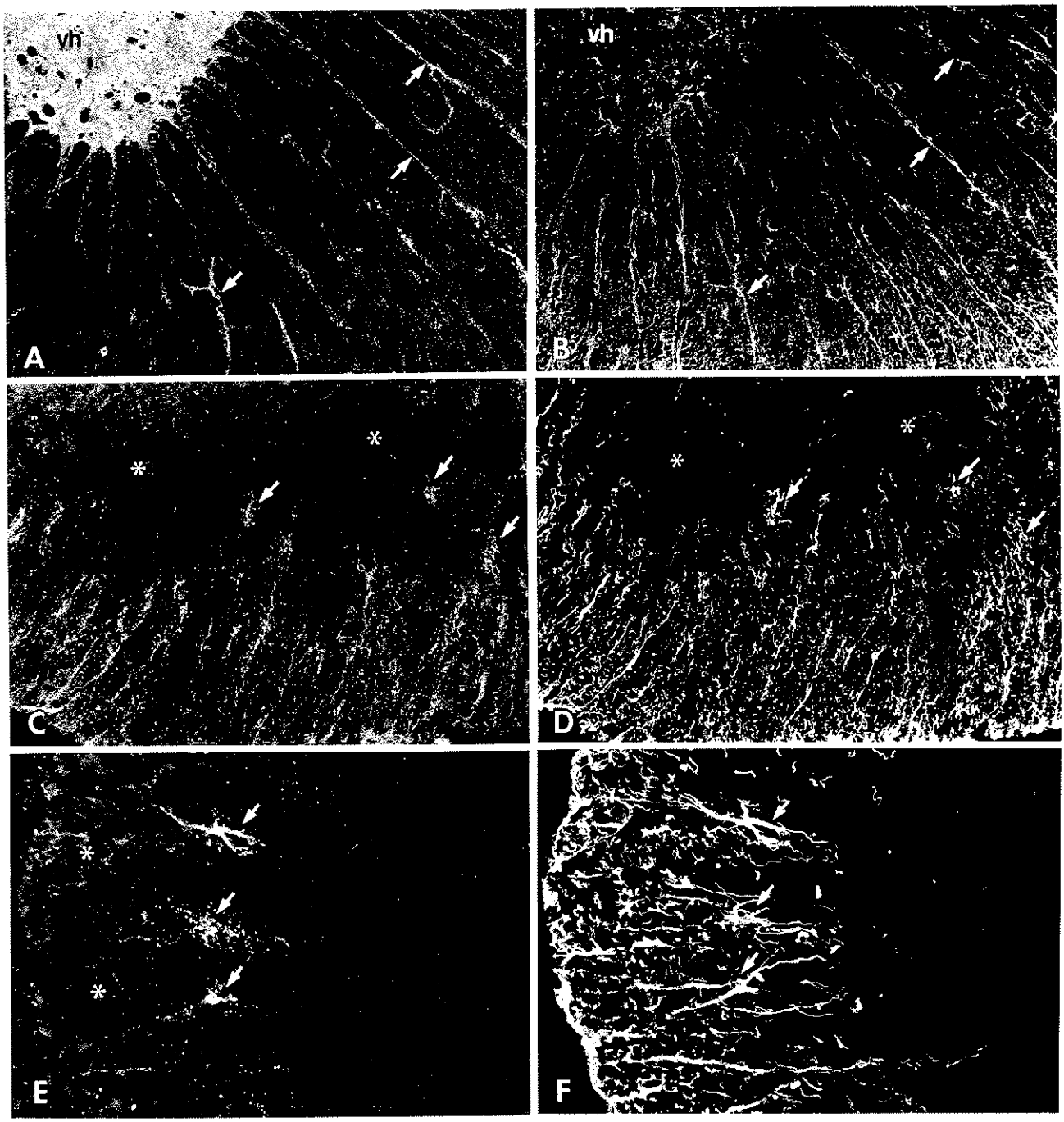

Fig.12

VII. Figure 13

Fig. 13. Labelling for Cx43 and GFAP in lateral white matter near a crush site at 7 days post-injury. Pairs of immunofluorescence micrographs (A,B; C,D) show the same fields stained for Cx43 (A,C) and GFAP (B,D). **A-D:** All grey matter and central regions of white matter is devoid of Cx43 and GFAP labelling (asterisks). More peripherally, punctate staining for Cx43 (A) is uniformly present in areas containing GFAP-positive astrocytes (B) or is associated with centrally directed blood vessels (C, arrows; shown at higher magnification in E) laden with GFAP-positive fibers (D, arrows). Magnifications: A,B x120; C, x120; D, x120; E, x110.

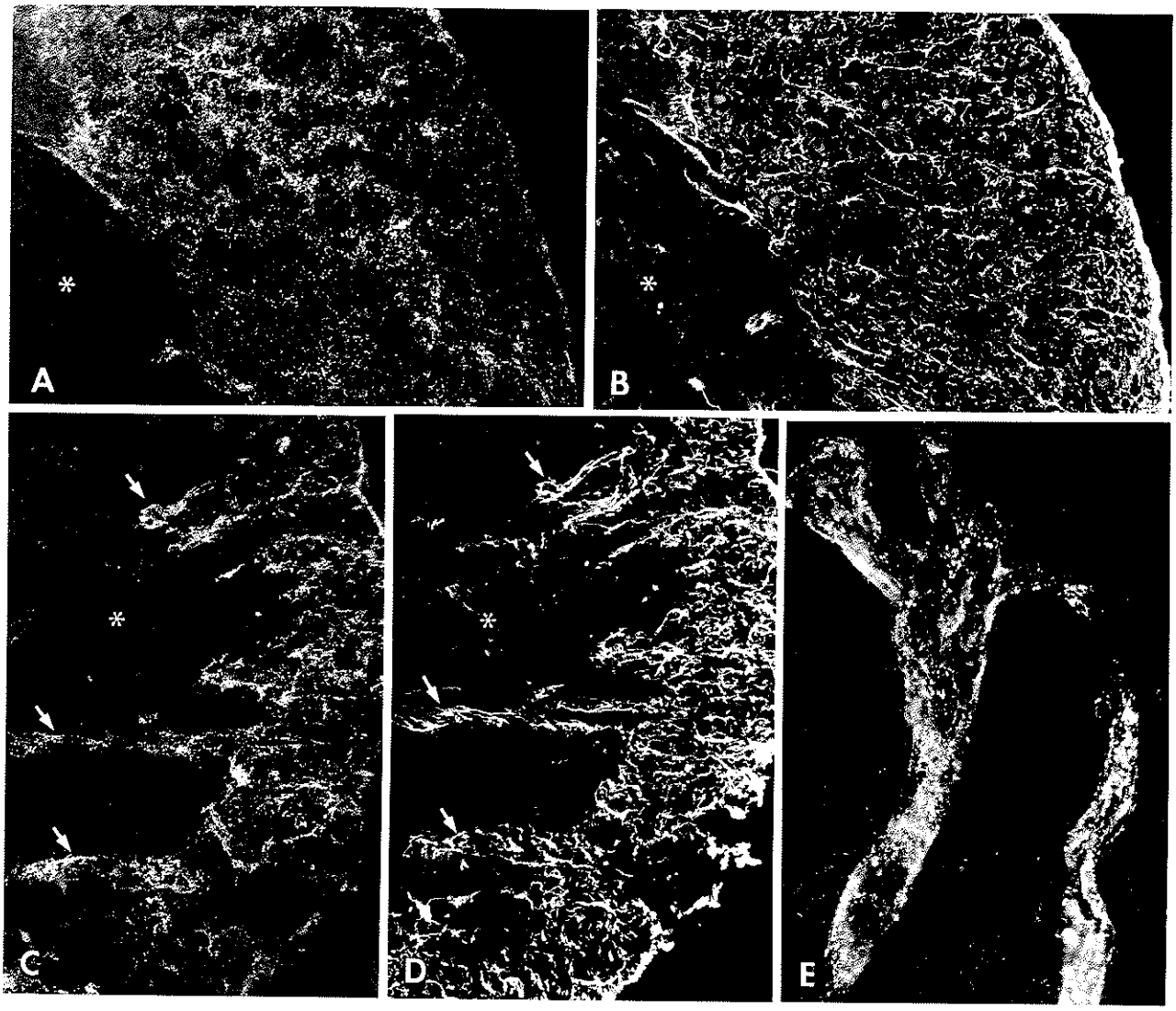

Fig.13

VII. Figure 14

Fig. 14. Comparison of Cx43-IR in normal cord white matter with similar areas at further distances from the crush site at 3 days survival time. **A:** Normal white matter showing association of Cx43 with bundles of fibers (arrows) eminating from the grey matter. **B:** In transverse sections at 1.5-4.5 mm from the crush site the association of Cx43 with bundles of myelinated fibers is decreased (arrows). Magnifications: A,B x50.

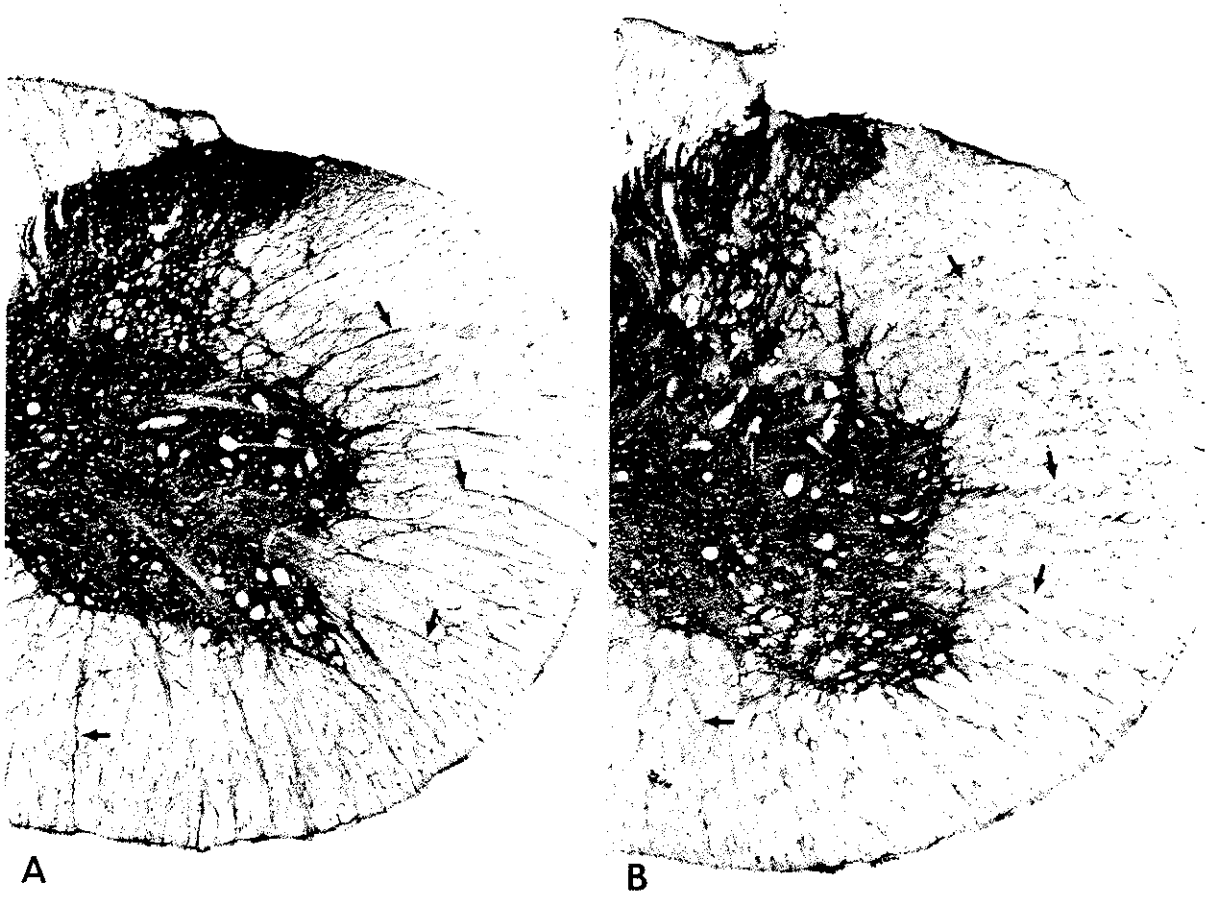

Fig.14

VIII. REFERENCES

el Aoumari, A., Fromaget, C., Dupont, E., Reggae, H., Durban, P., Brained, J.P., Bolero, K., Kreitman, B. and Gros, D. (1990) Conservation of a cytoplasmic carboxy-terminal domain of connexin43, a gap junctional protein, in mammal heart and brain. J. Membr. Biol.,115:229-240.

Batter, D.K., Corpina, R., Roy, C., Spray, D.C., Hertzberg, E.L. and Kessler, J.A. (1992) Heterogeneity in gap junction expression in astrocytes cultured from different brain regions. Glia, 6:213-221.

Belin, V. and Moos, F. (1986) Paired recordings from supraoptic and and paraventricular oxytocin cells in suckled rats: recruitment and synchronization. J. Physiol., 377:369-390.

Belliveau, D.J., Kidder, G.M. and Naus, C.C. (1991) Expression of gap junction genes during postnatal neural development. Dev. Genet., 12:308-317.

Bennett, M.V.L. (1977). Electrical transmission: a functional analysis and comparison with chemical transmission. In "Handbook of Physiology, Section 1: The Nervous System" (E. R. Kandel, ed.), pp.357-416. Williams and Wilkins, Baltimore.

Bennett, M.V.L., Barrio, L.C., Bargiello, T.A., Spray, D.C., Hertzberg, E.L. and Saez, J.C. (1991) Gap junctions: new tools, new answers, new questions. Neuron,6:305-320.

Bennett, M.V.L. and Goodenough, D.A. (1978) Gap junctions, electrotonic coupling and intercellular communication. Neurosci. Res. Prog. Bull., 16:376-486.

Beyer, E.C. (1993) Gap junctions. Int. Rev. Cyt., 137C:1-37.

Beyer, E.C. (1990) Connexin family of gap junction proteins. J. Membrane Biol., 116:187-194.

Beyer, E.C., Paul, D.L. and Goodenough, D.A. (1987) Connexin43: A protein from rat heart homologous to a gap junction protein in liver. J. Cell Biol., 105:2621-2629.

Bodega, G., Fernandez, B., Suarez, I. and Gianonatti, C. (1986) Glioarchitectonics of the rat spinal cord. J. Hirnforsch., 27:577-585.

Connors, B.W., Benardo, L.S. and Prince, D.A. (1984) Carbon dioxide sensitivity of dye coupling among glia and neurons of the neocortex. J. Neurosci., 4:1324-1330.

Dermietzel, R. and Spray, D.C. (1993) Gap junctions in the brain: where, what type, how many and why? Trends Neurosci, 16:186-192.

Dermietzel, R., Hertzberg, E.L., Kessler, J.A. and Spray D.C. (1991) Gap junctions between cultured astrocytes: immunocytochemical, molecular, and electrophysiological analysis. J. Neurosci., 11:1421-1432.

Dermietzel, R., Traub, O., Hwang, T.K., Beyer, E., Bennett, M.V.L., Spray, D.C. and Willecke, K. (1989) Differential expression of three gap junction proteins in developing and mature brain tissues. Proc. Natl. Acad. Sci. U.S.A., 86:10148-10152.

Dermietzel, R., Yancey, S.B., Traub, O., Willecke, K. and Revel, J.P. (1987) Major loss of the 28-kD protein of gap junction in proliferating hepatocytes, J. Cell Biol., 105:1925-1934.

Dudek, F.E., Gribkoff, V.K., Olson, J.E. and Hertzberg, E.L. (1988) Reduction of dye coupling in glial cultures by microinjection of antibodies against the liver gap junction polypeptide. Brain Res., 439:275-280.

Dudek, F.E., Andrew, R.D., MacVicar, B.A., Snow, R.W. and Taylor, C.P. (1983) Recent evidence for and possible significance of gap junctions and electrotonic synapses in the mammalian brain. In: Basic Mechanisms of Neuronal Hyperexcitability (H.H. Jasper and N.M. van Gelder, eds.) New York, Liss, pp. 31-73.

Dupont, E., el Aoumari, A., Fromaget, C., Brained, J.P. and Gros, D. (1991) Affinity purification of rat junctional protein, connexin43. Eur. J. Biochem., 200:263-270.

Dusart, I. and Schwab, M.E. (1994) Secondary cell death and the inflammatory reaction after ndorsal hemisection of the rat spinal cord. Eur. J. Neurosci., 6:712-724.

Ebihara, L., Beyer, E.C., Swenson, K.I., Paul, D.L. and Goodenough, D.A. (1989) Cloning and expression of a xenopus embryonic gap junction protein. Science, 243:1194-1195.

Eddelston, M. and Mucke, L. (1993) Molecular profile of reactive astrocytes- implications for their role in neurological disease. Neuroscience, 54:15-36.

Finch, E.A. and Paul, D.C. (1989) Expression and localization of different gap junction proteins in retina and other regions of the CNS. Soc. Neurosci. Abstr., 15, 127.

Fischer, G. and Kettenmann, H. (1985) Cultured astrocytes form a syncytium after maturation. Exp. Cell Res., 159:273-279.

Franklin, W.A. and Locker, J.D. (1981) Ethidium bromide: a nucleic acid stain for tissue sections. J. Histochem. Cytochem., 4:572-576.

Fursphan, E.J. and Potter, D.D. (1959) Transmission of the giant motor synapses of the crayfish. J. Physiol. (London) 145:289-325.

Gardner-Medrin, A.R. (1986) A new framework for assessment of potassium-buffering mechanisms. Ann. NY Acad. Sci., 481:287-301.

Giaume, C., Fromaget, C., el Aoumari, A.E., Cordier, J., Glowinski, J. and Gros, D. (1991) Gap junctions in cultured astrocytes: single-channel currents and characterization of channel-forming protein. Neuron, 6:133-143.

Gimlich, R.L., Kumar, N.M. and Gilula, N.B. (1988) Sequence and developmental expression of mRNA coding for gap junction protein in xenopus. J. Cell Biol., 1107:1065-1073.

Gutnick, M.J., Connors, B.W. and Ransom, B.R. (1981) Dye-coupling between glial cells in the guinea pig neocortical slice. Brain Res., 213:486-492.

Haeflinger, J.A., Bruzzone, R., Jenkens, N.A., Gilbert, D.J., Copeland, N.G. and Paul, D.L. (1992) Molecular cloning, expression, and chromosome mapping. J. Biol. Chem., 267:2057-2064.

Hajos, F. and Kalman, M. (1989) Distribution of glial acidic protein (GFAP)-immunoreactive astrocytes in the rat brain. Exp. Brain Res., 78:164-173.

Hatton, G.I. and Yang, Q.Z. (1990) Activation of excitatory amino acid inputs to supraoptic neurons. I. Induced increases in dye-coupling in lactating, but not virgin or male rats. Brain Res., 513:264-269.

Hertzberg, E.L., Lawrence, T.S. and Gilula, N.B. (1981) Gap junctional communication. Ann. Rev. Physiol., 43:479-491.

Hoh, J.H., John, S.A. and Revel, J.-P. (1991) Molecular cloning and characterization of a new member of the gap junction gene family, connexin31. J. Biol. Chem., 266:6524-6531.

Hossain, M.Z., Sawchuk, M.A., Murphy, L.J., Hertzberg, E.L. and Nagy, J.I. (1994a) Kainic acid induced alterations in antibody recognition of Connexin43 and loss of astrocytic gap junctions in rat brain. Glia, 10:250-265.

Hossain, M.Z., Murphy, L.J., and Nagy, J.I. (1994b) Phosphorylated forms of connexin43 predominate in rat brain: Demonstration by rapid inactivation of brain metabolism. J. Neurochem., 62:2394-2403.

Hossain, M.Z., Peeling, J., Sutherland, G.R., Hertzberg, E.L. and Nagy, J.I. (1994c) Ischemia-induced cellular redistribution of the astrocytic gap junctional protein connexin43 in rat brain. Brain Res., 652:311-322.

Kettenmann, H. and Ransom, B.R. (1988) Electrical coupling between astrocytes and between oligodendrocytes studied in mammalian cell cultures. Glia, 1:64-73.

Kettenmann, H., Orkand, R.K. and Schachner, M. (1983) Coupling among identified cells in mammalian nervous system. J. Neurosci., 3:506-516.

Kumar, N.M. and Gilula, N.B. (1986) Cloning and characterization of human and rat liver cDNAs coding for a gap junction protein. J. Cell Biol., 103:767-776.

Larsen, W.J., Tung, H.N., and Polking, C. (1981) Response of granulosa cell gap junctions to human chorionic gonadotropin (hCG) at ovulation. Biol. Reprod., 25:1119-1123.

Lennette, D.A. (1977) An improved mounting medium for immunofluorescence microscopy. A. J. C. P., 69:647-648.

LePeq, J.B. (1971) Use of ethidium bromide for separation and determination of nucleic acids of various conformational forms and measurement of their associated enzymes. Methods Biochem. Anal., 20:41.

Liuzzi, F.J. and Miller, R.H. (1987) Radially oriented astrocytes in the normal adult rat spinal cord. Brain Res.,403:385-388.

Llinas, R.R. (1985) In: Gap junctions (Bennett M. V. L. and Spray, D. C. eds.) pp. 337-353, Cold Harbor Press.

Llinas, R.R., Grace, A.A. and Yarom, Y. (1991) In vitro neurons in mammalian cortical layer 4 exhibit intrinsic oscillatory activity in the 10- to 50-Hz frequency range. Proc. Natl. Acad. Sci. USA, 88:897-901.

Loewenstein, W.E. (1981) Junctional intercellular communication: the cell-to-cell membrane channel. Phys. Rev., 61: 829-913.

Loewenstein, W.E., Kanno, Y., and Socolar, S.J. (1978) Quantum jumps of conductance during formation of membrane channels at cell-cell junction. Nature, 274:133-136.

Maldonado, P.E., Rose, B. and Loewenstein, W.R. (1988) Growth factors modulate junctional cell-to-cell communication. J. Membrane Biol., 106:203-210.

Makowski, L., Caspar, D.L.D., Phillips, W.C. and Goodenough, D.A. (1977) Gap junction structures II. Analysis of the x-ray diffraction data. J. Cell Biol., 74:605-628.

Massa, P.T. and Mugnaini, E. (1982) Cell junctions and intramembrane particles of astrocytes and oligodendrocytes: a freeze-fracture study. Neuroscience, 7:523-538.

Matsumoto, A., Arai, Y., Urano, A. and Hyodo, S. (1991b) Androgen regulates gap junction mRNA expression in androgen-sensitive motoneurons in the rat spinal cord. Neurosci. Lett., 131:159-162.

Micevych, P.E. and Abelson, L. (1991) Distribution of mRNAs coding for liver and heart gap junction proteins in the rat central nervous system. J. Comp. Neurol., 305:96-118.

Miragall, F., Hwang, T.-K., Traub, O., Hertzberg, E.L. and Dermietzel, R. (1992) Expression of connexins in the developing olfactory system of the mouse. J. Comp. Neurol., 325:359-378.

Mugnaini, E. (1986) Cell junctions of astrocytes, ependyma, and related cells in mammalian central nervous system, with emphasis on the hypothesis of a generalized functional syncytium of supporting cells. In: "Astrocytes", Vol. 1, (S. Fedoroff and A. Verndakis, eds.), Academic Press, New York, pp 329-371.

Nagy, J.I., Yamamoto, T., Sawchuk, M.A., Nance, D.M. and Hertzberg, E.L. (1992) Quantitative immunohistochemical and biochemical correlates of connexin43 localization in brain. Glia, 5:1-9.

Nagy, J.I., Yamamoto, T., Shiosaka, S., Dewar, K.M., Whittaker, M.E. and Hertzberg, E.L. (1988) Immunohistochemical localization of gap junction protein in rat CNS: A preliminary account. In: Modern Cell Biology, Vol. 7. (E.L. Hertzberg and R.G. Johnson, eds.), Alan R. Liss Inc., New York, pp. 375- 389.

Naus, C.C.G., Belliveau, D.J. and Bechberger, J.F. (1990) Regional differences in connexin32 and connexin43 messenger RNAs in rat brain. Neurosci. Lett., 111:297-302.

Ochalski, P.A.Y., Sawchuk, M.A., Hertzberg, E.L. and Nagy, J.I. (1995) Astrocytic gap junction removal, connexin43 redistribution and epitope masking at excitatory amino acid lesion sites in rat brain. Glia, in press.

Paul, D. (1986) Molecular cloning of cDNA for rat liver gap junction protein. J. Cell Biol., 103:123-134.

Peracchia, C. (1980) Structural correlates of gap junction permeation. Int. Rev. Cytol., 66:81-146.

Pitts, J.D. (1978) Junctional communication and cellular growth control. In: "Intercellular junctions and Synapses" (J. Feldman, N. B. Gilula, J. D. Pitts, eds.), pp.61-80. Chapman and Hall, London.

Randriamampita, C., Giaume, C. and Trautmann, A. (1988) Acetylcholine-induced closure of gap junction channels in rat lacrimal glands is probably mediated by protein kinase C. Pflugers Arch., 412:462-468.

Ransom, B.R. and Kettenmann, H. (1990) Electrical coupling, without dye coupling, between mammalian astrocytes and oligodendrocytes in cell culture. Glia, 3:258-266.

Rethelyi, M. (1987) Spinal cord organization. In "Encyclopedia of Neuroscience" (G. Adelman, ed.), Birkhauser Boston Inc., Boston, pp.1128-1131.

Revel, J.P. and Karnovsky, M.J. (1967) Hexagonal array of subunits in intercellular junctions of the mouse heart and liver. J. Cell Biol., 33:C7-18.

Rup, D.M., Veenstra, R.D., Wang, H.Z., Brink, P.R. and Beyer, E.C. (1993) Chick connexin-56, a novel lens gap junction protein. Molecular cloning and functional expression. J. Biol. Chem., 268:706-712.

Robertson, J.D. (1963) The occurrence of a subunit pattern in the unit membranes of club endings in mauthner cell synapses in goldfish brains. J. Cell Biol.,19:201-221.

Rohlmann, A., Laskawi, R., Hofer, A., Dermietzel, R. and Wolff, J.R. (1994) Astrocytes as rapid sensors of peripheral axotomy in the facial nucleus of rats. Neuroreport, 5:409-12.

Rohlmann, A., Laskawi, R., Hofer, A., Dobo, E., Dermietzel, R. and Wolff, J.R. (1993) Facial nerve lesions lead to increased immunostaining of the astrocytic gap junction protein (connexin43) in the corresponding facial nucleus of rats. Neurosci. Lett., 154:206-208.

Saez, J.C., Spray, D.C., Nairn, A.C., Hertzberg, E.L., Greengard, P. and Bennett, M.V.L. (1986) cAMP increases junctional conductance and stimulates phosphorylation of the 27-kDa principal gap junction polypeptide. Proc. Natl. Acad. Sci. USA, 83:2473-2477.

Sawchuk, M.A., Hossain, M.Z., Hertzberg, E.L. and Nagy, J.I. (1995) In situ transblot and immunocytochemical comparisons of astrocytic connexin43 responses to NMDA and kainic acid in rat brain. Brain Res., in press.

Schmued, L.C., Swanson, L.W. and Sawenchko, P.E. (1982) Some fluorescent counterstains for neuroanatomical studies. J. Histochem. Cytochem., 30:123-128.

Schwartzkroin, P.A. and Prince, D.A. (1979) Recordings from presumed glial cells in the hippocampal slice. Brain Res., 161:533-538.

Sipe, J.C. and Moore, R.Y. (1976) Astrocytic gap junctions in the rat lateral hypothalamic area. Anat. Rec., 185:247-252.

Sotelo, C. and Korn, H. (1978) Morphological correlates of electrical and other interactions through low-resistance pathways between neurons of the vertebrate central nervous system. Int. Rev. Cyt., 55:67-107.

Spray, D.C. and Bennett, M.V.L. (1985) Physiology and pharmacology of gap junctions. Ann. Rev. Physiol., 47:281-303.

Tator, C.H., and Fehlings, M.G. (1991) Review of the secondary injury theory of acute spinal cord trauma with emphasis on vascular mechanisms. J. Neurosurg., 75:15-26.

Theriault, E. and Tator, C. (1994) Persistence of rubrospinal projections following spinal cord injury in the rat. J. Comp. Neurol., 342:249-258.

Valnes, K. and Brandtzaeg, P. (1985). Retardation of immunofluorescence fading during microscopy. J. Histochem. Cytochem., 33:755-761.

Vukelic, J.I., Yamamoto, T., Hertzberg, E.L. and Nagy, J.I. (1991) Depletion of connexin43-immunoreactivity in astrocytes after kainic acid-induced lesions in rat brain. Neurosci. Let., 130:120-124.

Walz, W. (1989) Role of glial cells in the regulation of the brain ion microenvironment. Prog. Neurobiol., 33:309-333.

Waxman, S.G. and Black, J.A. (1984) Freeze-fracture ultrastructure of the perinodal astrocyte and associated glial junctions. Brain Res., 308:77-87.

Weidmann, S. (1952) The electrical constants of purkinje fibers. J. Physiol., 118:348-60.

Willecke, K., Heynkes, R., Dahl, E., Stutenkemper, R., Hennemann, H., Jungbluth, S., Suchyna, T. and Nicholson, B.J. (1991) Mouse connexin37: Cloning and functional expression of a gap junction gene highly expressed in lung. J. Cell Biol., 114:1049-1057.

Willecke, K., Jungbluth, S., Dahl, E., Hennemann, H., Heynkes, R. and Grzeschick, K.-H. (1990) Six genes of the human connexin gene family coding for gap junctional proteins are assigned to four different human chromosomes. Eur. J. Cell Biol., 53:275-280.

Wolpert, L. (1978) Gap junctions: channels for communication in development. In: "Intercellular junctions and Synapses" (J. Feldman, N. B. Gilula, J. D. Pitts, eds.), pp.83-94. Chapman and Hall, London.

Yamamoto, T., Hertzberg, E.L. and Nagy, J.I. (1991) Subsurface cisterns in α-motoneurons of the rat and cat: immunohistochemical detection with antibodies against connexin32. Synapse, 8:119-136.

Yamamoto, T., Ochalski, A., Hertzberg, E.L. and Nagy, J.I. (1990a) On the organization of astrocytic gap junctions in rat brain as suggested by LM and EM immunohistochemistry of connexin43 expression. J. Comp. Neurol., 302:853-883.

Yamamoto, T., Ochalski, A., Hertzberg, E.L. and Nagy J.I. (1990b) LM and EM immunolocalization of the gap junctional protein Connexin43 in rat brain. Brain Res., 508:313-319.

Yamamoto, T., Shiosaka, S., Whittaker, M.E., Hertzberg, E.L. and Nagy, J.I. (1989) Gap junction protein in rat hippocampus: Light microscope immunohistochemical localization. J. Comp. Neurol., 281:262-281.

Yang, Q.Z. and Hatton, J.I. (1988) Direct evidence for electrical coupling among rat supraoptic nucleus neurons. Brain Res., 463:47-56.

Yee, A. and Revel, J.-P. (1978) Loss and reappearance of gap junctions in regenerating liver. J. Cell Biol., 78:554-564.

Zhang, J.T. and Nicholson, B.J. (1989) Sequence and tissue distribution of a second protein of hepatic gap junctions, Cx26, as deduced from its cDNA. J. Cell. Biol., 109:3391-3401.